Version of Record: https://www.sciencedirect.com/science/article/pii/S0306261918316738
Manuscript_9bd88897c98c8eaffe45e546bb554497

The independent and coupled effects of feedstock characteristics and reaction conditions on biocrude production by hydrothermal liquefaction

David C. Hietala[a], Casey M. Godwin[b], Bradley J. Cardinale[b], Phillip E. Savage[a,c,*]

[a] *Department of Chemical Engineering, University of Michigan, 2300 Hayward Street, 3074 H.H. Dow Building, Ann Arbor, Michigan 48109, United States*
[b] *Cooperative Institute for Great Lakes Research, School for Environment and Sustainability, University of Michigan, 440 Church Street, 1556 Dana Building, Ann Arbor, Michigan 48109, United States*
[c] *Department of Chemical Engineering, The Pennsylvania State University, 160 Fenske Lab, University Park, Pennsylvania 16802, United States*

Abstract

We examined the independent and coupled effects of temperature (150 to 350 °C), reaction time (1 to 100 min), slurry concentration (30 and 120 g L_{rxn}^{-1}), biochemical composition (5.2 to 28.5 wt% lipid, 14.7 to 50.9 wt% protein), and species identity (*Nannochloropsis*, *Chlorella*, and *Spirulina*) on the yield and composition of biocrude oil produced by hydrothermal liquefaction. Measured properties included gravimetric yield, elemental (C, H, N, S, O, and P) composition and recovery, higher-heating value and energy recovery, and fatty-acid profile, content, and recovery. All examined factors affect the yield and composition of the biocrude, with biochemical composition and temperature exhibiting the greatest impacts. We probed the effects of slurry concentration and species identity over numerous combinations of temperature, reaction time, and biochemical composition that were previously unexamined, demonstrating the effects of both slurry concentration and species identity to be of the same order of magnitude as reaction time. Increased slurry concentration appears to promote Maillard reactions that result in increased biocrude yield, C content, and N content and decreased O content. Moreover, the extent of these Maillard reactions may be affected by the ratio of proteins to carbohydrates, with carbohydrates serving as the limiting reactant. High-lipid, 30 g L_{rxn}^{-1} slurries reacted at 300 °C for 3.2 min (including 1 min heat-up) generally yielded more biocrude with higher C and H content and lower N, S, and O content than did their high-protein, 120 g L_{rxn}^{-1}, 200 °C, or 31.6 min counterparts. This condition also provided recoveries of saturated, monounsaturated, and polyunsaturated fatty acids in the biocrude of up to 89.3, 80.1, and 64.7 wt%, respectively, demonstrating for the first time that fast hydrothermal liquefaction can be an effective means of recovering high-value unsaturated fatty acids. The results and expansive experimental data herein provide a deeper level of understanding for microalgal hydrothermal liquefaction, enabling a greater extent of reaction engineering for the process than previously possible.

Keywords: hydrothermal liquefaction, microalgae, reaction conditions, concentration, biochemical composition, species identity

© 2018 published by Elsevier. This manuscript is made available under the Elsevier user license
https://www.elsevier.com/open-access/userlicense/1.0/

1. Introduction

The creation and implementation of renewable fuels is vital for mitigating the rise of atmospheric carbon dioxide concentrations and associated effects of climate change. Microalgae are an intriguing feedstock for these fuels because of their innate ability to grow on non-arable land, high photosynthetic efficiency and energy density compared to terrestrial biomass, and capability of facilitating wastewater treatment and nutrient recovery from agricultural systems [1–4].

Hydrothermal liquefaction (HTL) employs hot ($150 < T < 400$ °C), compressed ($5 < P < 250$ bar) water as the reaction medium to convert whole algal biomass into an energy-dense biocrude oil. Below around 225 °C, this process is sometimes referred to as hydrothermal carbonization [5]; however, temperatures this mild are also relevant for understanding the early stages of HTL. By employing water as the reaction medium, HTL eliminates energy expenditure for drying the biomass. Moreover, HTL exploits the properties of high-temperature water, including an increased ion product and decreased dielectric constant, to facilitate acid- and base-catalyzed reactions and solvate significantly less polar compounds than possible at ambient conditions, respectively [6]. Water under these conditions decomposes the lipid, protein, and carbohydrate biomolecules into smaller ones that further react, at times with water or each other, to form organic-phase-soluble (biocrude) and water-soluble compounds in addition to some solid and gas products [7]. Given that the whole algal biomass is converted, the biocrude oil contains tens of thousands of compounds spanning a variety of chemical classes. As an example, fatty acids, originating from the lipid fraction of the biomass, are some of the most highly desired components in the biocrude due to their long methylene chains; whereas, cyclic organic compounds containing heteroatoms, such as nitrogen, oxygen, and sulfur, are some of the lowest-quality components. Due to the variability in the composition of the compounds in biocrude oil, catalytic upgrading is required to improve biocrude quality before it can be processed in existing refineries [8–10]. For algal biofuels to be commercially viable, it is pivotal that the efficiencies of biocrude production via HTL and subsequent catalytic upgrading are maximized [11].

Biocrude yield and the extent of upgrading required depend on factors such as temperature and time [12–20], concentration [12, 14, 15, 21, 22], biochemical composition [18, 23–29], and species identity [24, 27]. Many previous studies of these factors have various limitations, however. Long heat-up times (> 3 min) frequently observed in previous studies [12–14, 17] obfuscated the independent effects of temperature and time. More recently, the kinetics of biocrude production via HTL have been demonstrated to occur on the timescale of seconds at temperatures of 300 °C [19]. It is therefore imperative that heat-up time is minimized to facilitate kinetic analyses at these temperatures. Concentration has generally been regarded as less influential than temperature and time, although it has usually only been examined at a single temperature and holding

*Corresponding author. Tel.: +1-814-867-5876; Fax: +1-814-865-7846
Email addresses: hietala@umich.edu (David C. Hietala), psavage@psu.edu (Phillip E. Savage)

time [12, 14, 15, 22]; without a comprehensive examination of concentration effects at a variety of reaction conditions, any conclusions about its effects should be viewed as tentative. Biochemical composition has been a subject of scrutiny at high reaction severity (temperature and time), but often only for one or two reaction conditions [23–29]. This factor remains relatively unexplored at low and mild reaction severities, which are regions of interest for kinetic analysis.

Given that species of algae exhibit wide-ranging differences in their proximate biomolecule composition (lipids, proteins, carbohydrates), the null expectation is that two species with similar biochemical composition would behave identically during HTL. In fact, previous studies employed linear regression for a variety of microalgae to demonstrate that differences in products via HTL at high reaction severity can be explained to a reasonable extent by differences in proximate biochemical composition [23, 26, 30]. However, the authors of the present study recently quantified the extent that species identity can further explain variation in biocrude yield and properties, and the effect of species identity was 11 to 40 % of that of biochemical composition depending on the biocrude property, for high reaction severity [27]. Variability in biocrude properties between different species, even after controlling for proximate biochemical composition, has been discussed previously [24], but is a subject that has received little scrutiny to date. During HTL at low-to-moderate reaction severity, differences in cell morphology, such as cell wall strength and surface-area-to-volume ratio, could be expected to affect the hydrothermal reactivity of microalgae, regardless of proximate biochemical composition. Even at high reaction severity, it is possible that proximate biochemical composition is insufficient for adequately correlating product characteristics, so observed differences due to species identity could also simply indicate that a more granular accounting of biomolecule composition (e.g., DNA, RNA, and unsaponifiable lipid contents) is necessary to explain the variation.

Importantly, these aforementioned factors are interrelated. For example, different classes of biomacromolecules hydrolyze at different rates as a function of reaction severity, producing numerous classes of degradation products [7]. With increasing slurry concentration, these degradation products may be relatively more likely to react with each other (e.g., the Maillard reaction between amino acids and reducing sugars) [31, 32]. Furthermore, even with the same biochemical composition, differences in cell wall resiliency to hydrothermal degradation [24] and possibly cell morphology between different microalgal species may affect their reactivity during HTL, depending on slurry concentration (more dilute means more exposure to high-temperature water) and reaction severity (more severe means faster degradation). No previous study has examined these factors together and how they may dynamically synergize or antagonize over regions of the reaction domain. Often times only a few of these factors are considered over a relatively narrow range of conditions, which limits the ability to broadly understand and ultimately model HTL kinetics.

In this study, we employ fast-heating batch reactors (1-min heat-up) to establish and corroborate the individual and synergistic impacts of several types of reaction conditions and feedstock characteristics on biocrude oil properties. Critically, we implement a design of experiments that evaluates the effect of each

independent variable alongside a variety of combinations of the other independent variables, rather than with a single, fixed set. As an example, this setup allows for the evaluation of concentration effects at low, medium, and high reaction severity for both high-lipid and high-protein biomass, which to date has not been presented in the literature. These experiments span reaction times logarithmically ($10^{0.0}$, $10^{0.5}$, $10^{1.0}$, $10^{1.5}$, and $10^{2.0}$ min) over a large range of temperatures (150, 200, 250, 300, and 350 °C) for six biomass types with different biochemical profiles (5.2 to 28.5 wt% lipid, 14.7 to 50.9 wt% protein) at two different slurry concentrations (30 and 120 g L_{rxn}^{-1}). The logarithmic scaling employed provides an equal number of measurements at both short reaction times ($<$ 10 min) and long reaction times ($\geq$ 10 min). Three of the biomass feedstocks, including a high-lipid *Nannochloropsis*, high-lipid *Chlorella*, and high-protein *Spirulina*, exhibit different proximate biochemical compositions, enabling the assessment of the effects of different lipid, protein, and carbohydrate contents at different reaction severities and slurry concentrations. The other three, including a high-protein *Nannochloropsis*, a high-protein *Chlorella*, and a mixture of high-protein *Spirulina* and high-lipid *Chlorella*, exhibit similar proximate biochemical composition, allowing assessment of the variability between different species over different reaction conditions and slurry concentrations while controlling for biochemical composition. Similarly, the two variants of *Nannochloropsis* and *Chlorella* allow evaluation of the effects of biochemical composition while controlling for species identity. Differences between the measured and predicted effects of the two-species mixture illuminate how the different proportions of biochemical components in high-protein *Spirulina* and high-lipid, high-carbohydrate *Chlorella* interact with each other over different reaction severities and slurry concentrations, compared to how they react individually. This article focuses on the impact of these inputs on the yield and composition of the biocrude oil, with that of the solid and gas fractions documented in the Appendices. These results provide a new level of insight into microalgal HTL, enabling more extensive process reaction engineering than possible before.

2. Materials and methods

2.1. Microalgae feedstocks

We obtained preservative-free high-protein *Nannochloropsis oculata* (Nan-1) as a slurry, high-lipid *Nannochloropsis salina* (Nan-2) as a dry powder, and *Spirulina platensis* (Spi-1) as a dry powder from commercial sources. We cultivated both a high-protein *Chlorella sorokiniana* (Chl-1) and high-lipid *Chlorella sorokiniana* (Chl-2) as 12-L batch cultures by manipulating nitrate concentration in the growth medium. See Section A.1.1 in Appendix A for additional information.

2.2. Slurry preparation

We diluted and pre-mixed each biomass type with deionized water to prepare slurries at a variety of mass percentages such that their concentrations were either 30 or 120 g L_{rxn}^{-1} at reaction conditions (150 to

350 °C). The solids content of those slurries ranged from 3.2 to 5.0 wt% and 11.6 to 17.3 wt%, respectively (Table A.1). We chose a mass per volume-at-reaction-condition basis for slurry concentration to allow for orthogonal comparison of temperature effects holding all else constant, which would not be possible using a wt% basis due to the expansion of water with increasing temperature. Moreover, a mass-per-volume basis is more relevant for characterizing reaction systems that deviate from first-order behavior. We note that all references to concentration herein, including those from the literature, are on this mass per volume-at-reaction-condition basis, *not* at ambient conditions. We prepared the two-species mixture slurries (Mix-m) by mixing roughly three parts low-protein *Chlorella* (Chl-2) with seven parts *Spirulina* (Spi-1) for an average Chl-2 content of 30.1 wt%. We calculated the predicted two-species mixture slurry (Mix-p) behavior based on the weighed average of the behavior of Spi-1 (69.9 wt%) and Chl-2 (30.1 wt%). See Section A.1.2 in Appendix A for additional information.

2.3. Hydrothermal liquefaction

We reacted 30 and 120 g L_{rxn}^{-1} slurries of all biomass types at 200 and 300 °C for 3.2 ($10^{0.5}$) and 31.6 ($10^{1.5}$) min . We also reacted 30 and 120 g L_{rxn}^{-1} slurries of Nan-1 and Chl-2 at 150, 250, and 350 °C for $10^{0.0}$, $10^{1.0}$, and $10^{2.0}$ min to probe a wider range of reaction severities. Moreover, we reacted 30 and 120 g L_{rxn}^{-1} slurries of Nan-2 and Spi-1 at 150 °C for 1 min and at 350 °C for 100 min to evaluate the effects of biochemical composition at the most mild and severe conditions; note that we excluded the 120 g L_{rxn}^{-1} slurry of Spi-1 at 350 °C due to excessively high viscosity. We conducted HTL at a total of 91 unique sets of reaction conditions in at least duplicate, and in some cases triplicate or more to generate enough product mass for subsequent analysis. All reactions were conducted in a completely random order.

We built each 1.30 mL batch reactor using 0.635-cm-o.d., 0.124-cm-thick Swagelok tubing cut to 10.5 cm lengths and two caps, all made of 316 stainless steel. We loaded each reactor with enough of the appropriate pre-mixed slurry such that 98 % of the control volume would be occupied at reaction conditions from thermal expansion under autogenous pressure. We sealed reactors to 27.1 Nm (20 ft-lb) using a torque wrench. We constructed additional 1.16 mL proxy reactors for temperature measurements using the same 10.5 cm lengths of tubing as the main reactors, a cap, and a 0.635-cm-to-0.159-cm bored-through reducing union. We fitted the reactors with an Omega Engineering 0.159-cm-diameter, 45.7-cm-long, stainless-steel-clad K-type thermocouple. We loaded proxy reactors with enough deionized water to match the same ratio of total-loaded-mass to-control-volume as the primary reactors. We used an Omega Engineering UWBT-TC-UST-NA Datalogger to record the temperature measured by the proxy reactor thermocouples every 1 s.

We conducted reactions individually by immersing both a slurry-loaded reactor and proxy reactor in a Techne IFB-51 fluidized sand bath, preheated to the specified temperature. It typically took reactors about 58 s to achieve 98% of the maximum temperature change. At a set-point temperature of 250 °C, for example,

this is a temperature change of change of 220.5 °C, or when the reactor reaches 245.5 °C. At the end of the holding time ($10^{0.0}$, $10^{0.5}$, $10^{1.0}$, $10^{1.5}$, or $10^{2.0}$ min), we quenched the reactors in a cold water bath. We define this holding time as the time from the moment the reactor starts to heat up to the moment the reactor starts to cool down.

We measured 5.5 mL of dichloromethane (>99.9% optima grade, Fisher Scientific) and enough deionized water (4.3 to 4.9 mL) such that the total volume of water (in the reaction mixture and added water) was approximately 5.5 mL to facilitate product collection via glass pipette. Following product recovery, we vortexed and centrifuged the product mixture to separate the biocrude (dichloromethane-soluble), aqueous, and solid products. We then dried those products under nitrogen (99.998%, Metro Welding Supply Corp.) at 35 °C for the biocrude and solid products and at 70 °C for the aqueous-phase products. See Section A.1.3 in Appendix A for additional HTL details, including representative heat-up profiles.

2.4. Fatty-acid esterification

We adapted the procedure used to extract, esterify, and quantify fatty acids from the method developed by Levine et al. [33]. Briefly, this method extracts and converts fatty acids to fatty acid methyl esters (FAMEs) by acid-catalyzed transesterification. We quantified FAMEs using gas chromatography with a flame ionization detector (GC-FID) and tricosanoic methyl ester (C23:0) as the internal and external standard. See Section A.1.4 in Appendix A for additional information regarding these methods.

2.5. Elemental content

Elemental Microanalysis Ltd measured C, H, N, and S content via the Dumas combustion method in duplicate on dry biomass feedstocks and as a single replicate on all other samples, as mass permitted. Elemental Microanalysis Ltd also directly measured biomass feedstocks for O content in duplicate via the Unterzaucher pyrolysis method, and we calculated O content for all other samples by difference. We measured total P in the algal biomass using persulfate digestion and the ascorbic acid molybdenum method [34, 35]. We measured P content in the solids and biocrude by combusting the samples at 550 °C for 4 h, dissolving the ash in hot 0.5 normal sulfuric acid for 8 h, and then using the ascorbic acid molybdenum method [36]. We measured absorbance using a Biotek Synergy H1 plate reader. We calculated biomass and biocrude higher-heating values (HHV) according to the formula developed by Channiwala and Parikh [37]. See Section A.1.5 in Appendix A for additional information, including biomass elemental composition data (Table A.4).

2.6. Biomass biochemical content

We estimated biomass lipid content as the total fatty-acid content of the biomass (see Section 2.4) averaged over five replicates, with the acknowledgement that unsaponifiable lipids and minor components

derived from the lipid structures, such as phosphate and glycerol, will be neglected. We estimated biomass protein content by multiplying biomass N content by 4.78, a standard multiplication factor averaged over all growth phases for a wide variety of types of microalgae [38]. We measured biomass ash content by combusting the samples at 550 °C for 30 h and calculating the percentage of mass retained, minus biomass P content, averaged over five replicates. We calculated biomass carbohydrate content by difference from unity and the sum of lipid, protein, and ash content. Table 1 lists the biochemical profiles, shorthand identifiers, and symbols (used in figures) for each of the biomass types incorporated in this study. Figure 1 presents color-coded ternary diagrams of these different biochemical profiles on a dry, ash-free basis, with the lipid, protein, and carbohydrate contents mapped to red, green, and blue intensity, respectively.

ID	Symbol	Genus	Biochemical Composition [wt%]			
			Lipid	Protein	Carb.	Ash
Nan-1	●	*Nannochloropsis*	11.6 ± 0.1	41.8	43.7	2.8 ± 0.6
Nan-2	●		28.5 ± 0.5	20.1	44.7	6.7 ± 0.9
Chl-1	■	*Chlorella*	9.4 ± 0.3	43.3	42.5	4.8 ± 0.9
Chl-2	■		19.9 ± 0.1	14.7	61.9	3.4 ± 0.5
Spi-1	⬟	*Spirulina*	5.2 ± 0.1	50.9	31.4	12.5 ± 1.3
Mix-m	▼	Mixture	9.6 ± 0.1	40.0	40.6	9.7 ± 1.1
Mix-p	▲		9.6 ± 0.1	40.0	40.6	9.7 ± 1.1

Table 1: Biomass type legend. Mix-m and Mix-p represent the measured and predicted values for the two-species mixture, respectively, and were calculated as an abundance-weighted average of Chl-2 and Spi-1. Uncertainty denotes standard error.

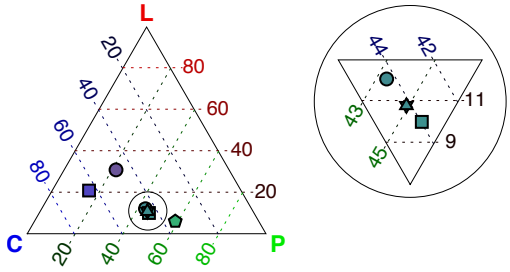

Figure 1: Biochemical profile ternary diagrams (dry, ash-free basis) of six different microalgal feedstocks presented in Table 1. L (red), P (green), and C (blue) denote color-shaded profile of lipids, proteins, and carbohydrates, respectively.

2.7. Statistical analysis

All statistical analyses on subsets of the data used the function `LocationTest` in Mathematica 11.1, which chooses the most powerful test to apply among the following: t-test, paired t-test, z-test, paired z-test, sign test, signed-rank test, and Mann-Whitney U test. When comparing two sets of data spanning two or more sets of reaction conditions, this tested the null hypothesis that the difference in those two sets had a true population mean or median of zero, and alternative hypothesis that they are nonzero. When

comparing data collected at just two different sets of reaction conditions, this tested whether the means or medians of the two sets of replicate data (which could be unequal in length if more than two replicates were run) were equal. All comparisons between subsets of the data are on an absolute deviation basis, not relative, unless otherwise stated.

3. Results and discussion

3.1. Biocrude yield

3.1.1. Temperature and time

Biocrude yield generally increased monotonically with increasing temperature and time, shown in Figure 2, consistent with a vast number of previous findings [12–20]. Nonetheless, this trend plateaued or reversed from 10 to 100 min at 350 °C; over this range, the biocrude yield from both concentrations of Chl-2 (■) decreased by on average 3.3 wt% ($p < 0.06$), and that of the 120 g L_{rxn}^{-1} slurry of Nan-1 (●) decreased by 4.1 wt% ($p < 0.09$). Several studies have shown similar decreases in biocrude yield at high severity [16, 19, 20, 39], suggesting that 350 °C and 100 min is around the point at which hydrothermal gasification begins to occur to a significant extent.

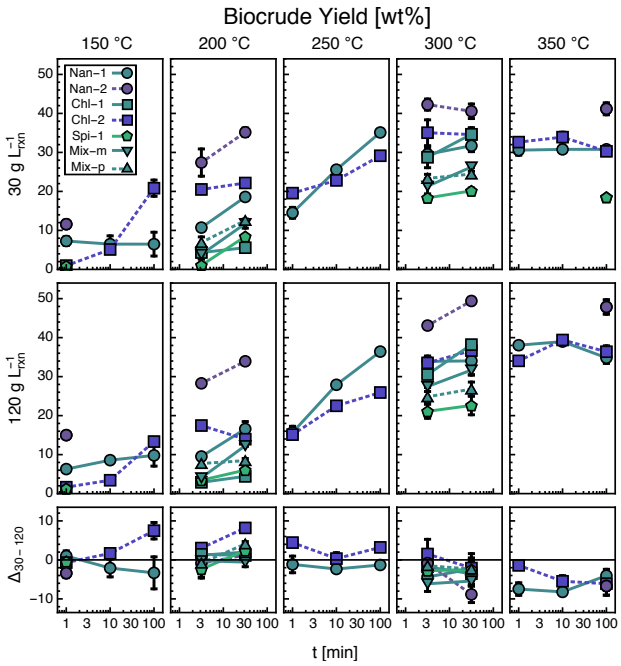

Figure 2: Biocrude yield versus reaction time grouped by temperature and initial concentration. See Table 1 for microalgae types. The bottom row depicts the first row (30 g L_{rxn}^{-1}) minus the second row (120 g L_{rxn}^{-1}). Error bars indicate standard error.

3.1.2. Slurry concentration

At several low-severity conditions (from 150 °C, 100 min to 250 °C, 1 min), the 30 g L_{rxn}^{-1} slurries of Chl-2 (▪) yielded on average 5.8 wt% ($p < 0.02$) more biocrude than the 120 g L_{rxn}^{-1} slurries. Moreover, this difference in biocrude yield was not accompanied by a statistically significant difference in mass closure (Fig. A.2), which varied by only 2.5 wt% ($p < 0.45$) on average. To the authors' knowledge, this effect of increased biocrude yield with decreasing concentration has not been demonstrated previously for microalgae, likely because it occurs at much lower reaction severities than those used by previous concentration studies [12, 14, 15, 21]. One possible explanation is that during product recovery, centrifugation extracted fatty acids from the degraded algal solids more efficiently for the less concentrated slurries. However, biocrude fatty-acid yields (Table B.7) in that range were only on average 1.8 % higher ($p < 0.06$) for 30 g L_{rxn}^{-1} slurries, so the increase in biocrude yield cannot be explained by fatty-acid yield alone. All elemental recoveries were higher, including N and S, suggesting that protein contributed as well, and perhaps carbohydrates. Given that Chl-1 (▪) did not experience the same magnitude of effect, it seems to be a result of biochemical differences rather than cell morphology.

At temperatures of 300 °C and higher, all biomass types generally trend toward significantly increased biocrude yield with increasing initial concentration, a finding which has been documented previously at these reaction conditions [12, 15, 21]. The absolute magnitude of this effect from 30 to 120 g L_{rxn}^{-1} is on average (across all species) about 3.4 wt% ($p < 0.006$) at 300 °C and 5.6 wt% ($p < 0.0007$) at 350 °C, with increases of up to 8.8 ± 2.1 wt% (Nan-2, ●, 300 °C, 31.6 min).

3.1.3. Biochemical composition

Increases in biomass lipid content generally were associated with increased biocrude yield (color-coded in Fig. 2; see Fig. B.1 in Appendix B for explicit yield vs. lipid content plots), which has been widely documented [18, 23–27, 29]. Controlling for reaction conditions and species identity, this was an increase of 11.1 wt% ($p < 10^{-6}$) on average (i.e., comparing the average difference in Nan-1 vs. Nan-2 and Chl-1 vs. Chl-2 across all reaction conditions). However, in several instances, the biocrude yields from the high-protein Nan-1 (●) and Chl-1 (▪) matched or exceeded those of the low-protein Chl-2 (▪). Although the latter contained more lipids than the other two, it also contained more carbohydrates as well, which individually contributes much less to biocrude formation than the other biochemical fractions [23, 40].

3.1.4. Species identity

Despite featuring similar biochemical compositions, Mix-m (▾), Nan-1 (●), and Chl-1 (▪) yielded significantly different amounts of biocrude after controlling for reaction conditions (Fig. 2). Even at high severity (300 °C and 31.6 min), where biocrude yield tends to plateau, the variability in yields from these biomass samples was on average ± 3.7 wt% across both concentrations. López Barreiro et al. [24] found

that biochemical composition alone was insufficient for correlating the biocrude yield from HTL of eight different types of microalgae at two sets of reaction conditions similar to those employed in this study. They proposed that species identity played a nontrivial role in affecting biocrude yield predictability. The information presented here supports the claim that species identity induces variability, suggesting that biochemical composition could predict biocrude yield to within ± 3.7 wt% at high severity. It is expected that morphological differences between species would play less of a role at high reaction severity, so the source of the variation would most likely be explained by more granular differences in biochemical composition, such as polar, non-polar, and unsaponifiable lipids for example. Hietala et al. [27] recently quantified the relative effects of species identity and biochemical composition on biocrude yield to be at most 1.9 and 12.6 wt%, respectively, for the HTL of 30 g L_{rxn}^{-1} slurries of six different species of microalgae at 350 °C, 20 min. At 300 °C and 31.6 min in the present study, variability in biocrude due to species identity (± 3.7 wt%) is about twice as large that of Hietala et al. [27], while the variability due to biochemical composition in the present study is on average ± 11.8 wt%, similar to our previous results.

3.1.5. Two-species mixture interactions

The measured (Mix-m, ▾) and predicted (Mix-p, ▴) biocrude yields for the 30 g L_{rxn}^{-1} two-species mixture agreed across all four reaction conditions (Fig. 2). However, the measured biocrude yields for the 120 g L_{rxn}^{-1} slurry (▾) were on average 3.8 wt% higher than predicted (▴, $p < 0.03$) for all but the 200 °C and 3.2 min condition. This was especially the case at 300 °C and 31.6 min, with a measured biocrude yield of 31.7 ± 1.2 wt% compared to a predicted value of 26.8 ± 1.8 wt%. These data suggest that reactions between the biochemical components of the two different species form additional and/or higher-molecular-weight biocrude components in the bulk high-temperature water; moreover, these reactions are likely occurring between the relatively higher concentration of lipids and/or carbohydrates in Chl-2 and the relatively higher concentration of protein in Spi-1. Higher-than-predicted biocrude yield from mixtures of feedstocks (including various biomass types and model compounds) with differing biochemical composition has been reported previously [28, 40–43] and will be discussed further in Section 3.4.

3.2. Carbon content and recovery

3.2.1. Temperature, time, slurry concentration, and biochemical composition

C content in the biocrude ranged from 62.4 to 76.8 wt%, shown in Figure 3a. It monotonically increased with increasing reaction severities at temperatures of 250 °C and higher, consistent with findings from previous studies at comparable reaction conditions [13–15, 17, 24]. Slurry concentration affected biocrude C content only on reaction-condition- and feedstock-specific bases. C content generally increased with increasing lipid content (and decreasing protein content), consistent with previous work [25, 26]. Controlling for species identity, the C content in the biocrude from higher-lipid microalgae was on average 3.8 wt% higher

($p < 0.0005$) than that of the lower-lipid microalgae in the 200 to 300 °C range, for all holding times and slurry concentrations. Notably, at 350 °C and 100 min, the C content of Nan-1 (●), Nan-2 (●), and Chl-1 (■) varied by only only 1.3 wt%, despite differing initial concentrations and biochemical compositions (in the case of Nan-2); this result is in line with some previous results [24]. In contrast, Biller and Ross [23] found that biocrude C content decreased from 73.3 to 68.1 wt % with increasing lipid content for 64 g L_{rxn}^{-1} slurries of four different species of microalgae (including *Nannochloropsis*, *Chlorella*, and *Spirulina*) at 350 °C and approximately 90 min total holding time. The *Nannochloropsis* and *Chlorella* in that study contained significantly less carbohydrate content than the four types used in this study, which could explain the differences, although the authors of that study measured carbohydrates directly while those of the present study estimated them by difference. However, the biochemical compositions for *Spirulina* in both studies were very similar and so were the C contents in the biocrude at those reaction conditions (73.3 vs. 73.2 wt%). These results together suggest that biochemical composition affects C content at all reaction conditions and that the magnitude of this effect changes at different reaction conditions depending on the relative proportions of each biochemical class.

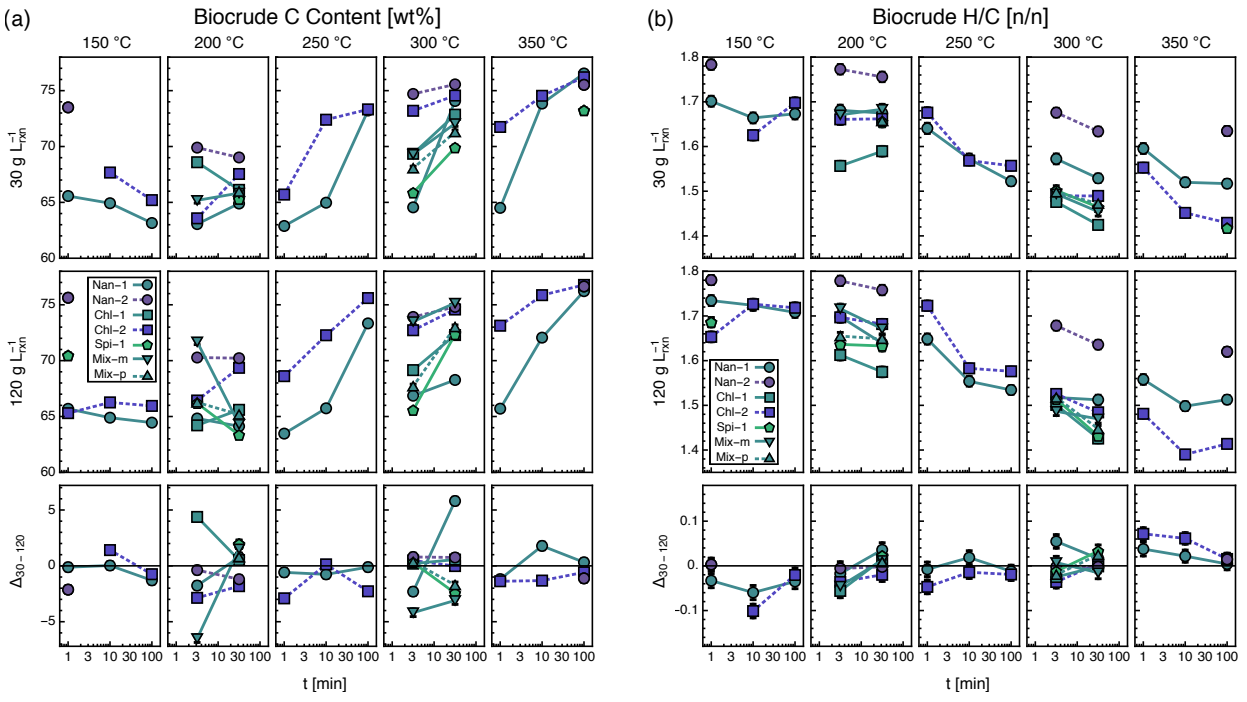

Figure 3: Biocrude (a) carbon content and (b) H/C ratio versus reaction time grouped by temperature and initial concentration. See Table 1 for microalgae types. The bottom row depicts the first row (30 g L_{rxn}^{-1}) minus the second row (120 g L_{rxn}^{-1}). Error bars indicate standard error.

3.2.2. Species identity and two-species mixture interactions

Biocrude C content varied significantly between Nan-1 (●), Chl-1 (■), and Mix-m (▼)—the three biomass types with similar biochemical composition—for low-severity (200 °C, 3.2 min) and high-severity (300 °C) conditions. At 300 °C across both reaction times and concentrations, the two-species mixture (▼) produced biocrude with C content that was on average 2.5 wt% higher ($p < 0.12$) than expected (▲). This was especially true for the 120 g L_{rxn}^{-1} slurry, which produced biocrude with C content that was on average 3.6 wt% higher ($p < 0.10$) than that of the 30 g L_{rxn}^{-1} slurry. Remarkably, the 120 g L_{rxn}^{-1} slurry featured biocrude C recovery, shown in Figure B.2, which was 8.1 % higher ($p < 0.08$) than predicted and 11.0 % higher ($p < 0.04$) than that of the 30 g L_{rxn}^{-1} slurry. These observations together suggest that reactions between the different biochemical components (and their degradation products) of the lipid- and carbohydrate-rich *Chlorella* and protein-rich *Spirulina* are actually improving carbon partitioning into the biocrude oil by forming more and/or higher-molecular-weight, carbon-containing, organic-phase-soluble compounds than predicted by reacting the equivalent proportion of both species individually. Madsen et al. [28] also observed increased biocrude C content for several 64 g L_{rxn}^{-1} biomass mixtures at 350 °C, 20 min, including a mixture of high-protein *Spirulina* and high-carbohydrate poplar wood with roughly the same overall biochemical composition as the mixture employed in this study.

3.3. Hydrogen content and recovery

H content in the biocrude, shown in Figure B.3a, did not follow any global trends with respect to changing temperature, time, and concentration. However, biocrude H recovery did generally increase with increasing temperature and time, shown in Figure B.3b, following the same general trends reported for biocrude yield in Section 3.1. Controlling for species identity and reaction conditions, increased biomass lipid content (and decreased protein content) resulted in an average of 1.1 wt% higher ($p < 0.0002$) H content across all reaction conditions, a trend similar to ones reported previously [25, 26]. Similar to C content, the 120 g L_{rxn}^{-1} two-species mixture produced biocrude with 0.5 wt % higher H content ($p < 0.1$) than expected at 300 °C.

Biocrude H/C (molar ratio of H to C), depicted in Figure 3b, generally decreased with increasing temperature and time, similar to previous reports [13]. Given that C and H recovery (Figures B.2 and B.3a) both increase with increasing reaction severity, the decrease in H/C suggests that the ratio of the net rates of partitioning of H and C into the biocrude also decreases with increasing reaction severity. This could be due to an increase in H leaving the biocrude and/or a decrease in H entering the biocrude, relative to the rate of C flux. There were no global effects of initial concentration on biocrude H/C, although it did increase on average by 0.09 ($p < 10^{-9}$) with increasing biomass lipid content, after controlling for species identity and reaction conditions, which corroborates prior findings [25, 26].

3.4. Nitrogen content

3.4.1. Temperature and time

Across the entire data set, biocrude N content varied from 0.3 to 8.4 wt%, shown in Figure 4a. It generally increased with increasing temperature and time, which is consistent with previous reports [12–15, 21]. Although at 300 °C and higher, there was no overall trend with respect to temperature and time, but there were trends within different biochemical profiles (see Section 3.4.3). Regardless of biomass type, at 200 °C and higher, the 120 g L_{rxn}^{-1} slurries produced biocrude with on average 0.47 wt% higher ($p < 10^{-9}$) N content than their 30 g L_{rxn}^{-1} counterparts. From 200 °C, 3.2 min to 300 °C, 3.2 min, this effect was only significant for the higher-protein biomass types and not the higher-lipid biomass samples, on average 0.64 ($p < 0.00003$) and 0.07 wt% ($p < 0.17$) higher, respectively. However, at 300 °C, 31.6 min and higher, the average effects were the same regardless of biochemical composition, at 0.56 ($p < 0.004$) and 0.55 wt% ($p < 0.001$) for higher-protein and higher-lipid biomass, respectively. It is not immediately clear why increased concentration promotes N partitioning into the biocrude, however one possibility is that it promotes the formation of dichloromethane-soluble N-containing compounds via Maillard reactions, or reactions between carbohydrate and protein degradation products [42]. Maillard reactions have been demonstrated to occur in high-temperature water [31, 44] and increase biocrude nitrogen content [28, 41, 45]. These reactions could be first order in both amino acids and saccharides (second order overall), so concentration increases would increase their selectivity during HTL.

3.4.2. Slurry concentration

To the authors' knowledge there is only one previous study that presented elemental content of biocrude oils as a function of slurry concentration [21]. It showed that at 300 °C and 3 min, biocrude N content increased from 7.2 to 7.8 wt% with an increase in slurry concentration from 37 to 79 g L_{rxn}^{-1} for a high-protein *Chlorella*, which is in line with the average increase observed in the present study. However, at 350 °C they reported a slight decrease in biocrude N of 7.9 to 7.7 wt% with concentration increasing from 30 to 64 g L_{rxn}^{-1}, which we did not observe. We note however that at that temperature, the concentration change herein was approximately double that of theirs (30 to 120 vs. 30 to 64 g L_{rxn}^{-1}), so it is possible that a fourfold increase in concentration, as was the case in the present study, is necessary to observe a significant concentration effect at 350 °C.

3.4.3. Biochemical composition

Biomass biochemical composition significantly affected biocrude N content (color-coded in Fig. 4a; see Fig. B.4a in Appendix B for explicit N content vs. protein content plots), which for example ranged from 2.3 to 8.4 wt% for 120 g L_{rxn}^{-1} slurries at 300 °C and 3.2 min. Controlling for species identity and reaction conditions, biocrude N content was on average 2.2 wt% higher ($p < 10^{-5}$) for higher-protein biomass types

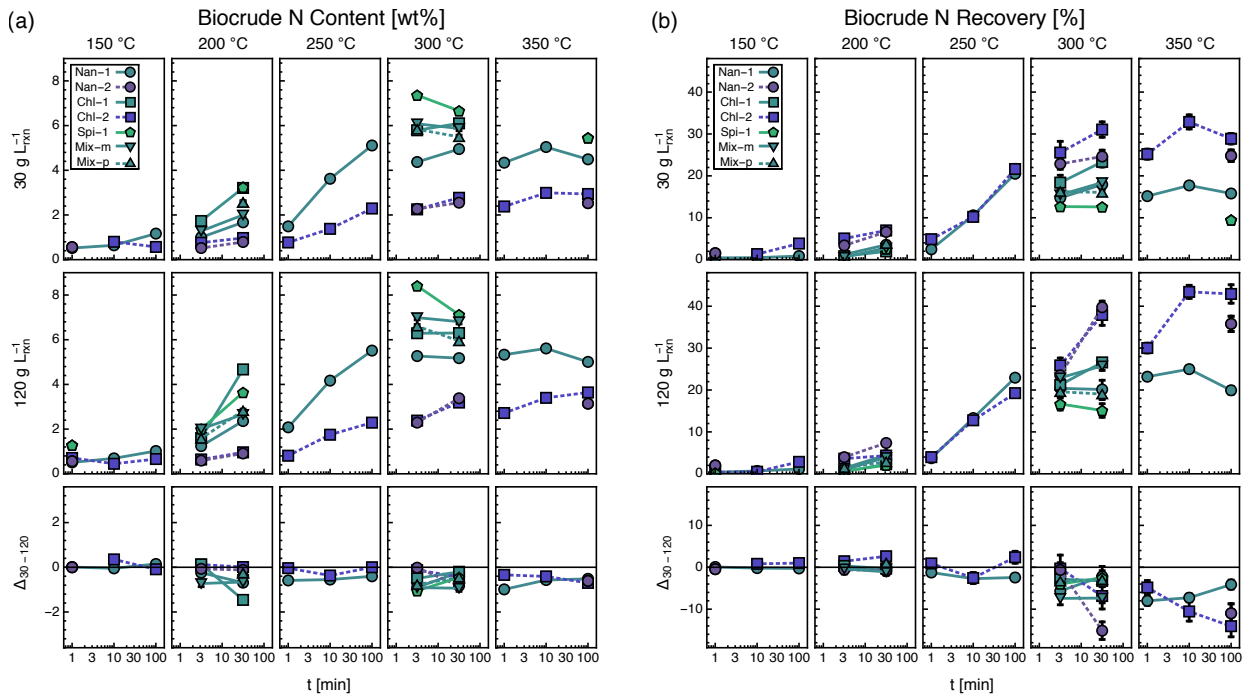

Figure 4: Biocrude nitrogen (a) content and (b) recovery versus reaction time grouped by temperature and initial concentration. See Table 1 for microalgae types. The bottom row depicts the first row (30 g L_{rxn}^{-1}) minus the second row (120 g L_{rxn}^{-1}). Error bars indicate standard error.

compared to lower-protein biomass samples at 200 °C and higher. Leow et al. [25] and Li et al. [26] showed that, when controlling for species identity, biocrude N content increased linearly with increasing biomass protein content for 178 g L_{rxn}^{-1} slurries at 300 °C, 30 min, which is consistent with the results presented here (Fig. B.4a). The levels of reaction severity at which biocrude N content plateaued and then decreased appears to have increased with decreasing protein content. For example, biocrude N content for the highest-protein-content type, Spi-1 (⬟), decreases with increasing time at 300 °C; this trend is consistent with reported decreases for a high-protein *Chlorella vulgaris* [20]. However, N content in biocrude from biomasses that are lower, but still high in protein content, including Nan-1 (●), Chl-1 (■), and Mix-m (▼), generally plateau at 300 °C, and that of the lowest in protein content, including Nan-2 (●) and Chl-2 (■), actually increases with increasing time at 300 °C. Therefore the reaction conditions for maximum N content in the biocrude appear to be a function of biochemical composition as well.

3.4.4. Species identity

Biocrude N content varied by as much as 2.3 wt% and as little as 0.7 wt% between the three biomass types with similar biochemical composition after controlling for reaction conditions. The measured two-species mixture (▼) biocrude N content was on average 0.47 wt% higher ($p < 0.10$) than predicted (▲) for all times and concentrations at 300 °C. The mixture contains both a high-protein *Spirulina* (Spi-1) and a high-

carbohydrate *Chlorella* (Chl-2), which suggests that Maillard reactions are likely to account for the difference between measured and predicted values. The presence of both protein- and carbohydrate-degradation products together has been shown to shift selectivities toward nitrogen-containing ring structures over cyclic oxygenates [28, 43] to the point where a 1:1 mixture of protein and carbohydrate model compounds, the latter of which contains no N, produces biocrude with nearly the same N content as that of pure protein. These cross reactions can also form N- and O-containing structures that are unique from those present in biocrude from pure feedstocks [41].

3.5. Nitrogen recovery

N recovery in the biocrude, shown in Figure 4b, followed trends with respect to temperature, time, and concentration that are similar to those of N content, consistent with previous reports [46, 47]. A maximum biocrude N recovery of 43.4 % occurred for the 120 g L_{rxn}^{-1} slurry of Chl-2 (▪) at 350 °C and 10 min. At 250 °C and higher, biocrude N recovery was on average 4.6 % higher (absolute, $p < 10^{-5}$) for the 120 g L_{rxn}^{-1} slurries than the 30 g L_{rxn}^{-1} slurries; the largest absolute increase in biocrude N recovery due to increasing concentration was 15.1 %, in the case of Nan-2 (●) at 300 °C and 31.6 min. The more highly concentrated (120 g L_{rxn}^{-1}) slurries of Mix-m (▼) at 300 °C also recovered 5.0 % ($p < 0.21$) more N in the biocrude than predicted (▲); whereas this effect was absent or significantly reduced for the 30 g L_{rxn}^{-1} slurries. Given that Maillard reactions between sugars and amino acids likely proceed by an overall second order reaction mechanism, we propose that the four-fold increase in concentration likely promoted these reactions and the higher biocrude N recovery observed or the 120 g L_{rxn}^{-1}.

Notably, the trends in N recovery in the biocrude due to changing biochemical composition are the opposite of those of N content (color-coded in Fig. 4b; see Fig. B.4b in Appendix B for explicit N recovery vs. protein content plots). In fact, after controlling for species identity, biocrude N recovery increased by 5.8 % (absolute, $p < 0.0005$) on average with decreasing protein content (and increasing lipid content) at 200 °C and higher. This is to say that although the mass percentage of N in biocrude is lower for lower-protein species, that N constitutes a higher percentage of the total N in the starting biomass than does the N from higher-protein species, an effect previously observed at 300 °C [25, 48]. This is significant because higher N recovery in the biocrude directly translates to lower N recovery in the aqueous phase for recycling. Amide derivatives have also been reported to increase with increasing lipid content and were in the range of 1.4 to 3.0 wt% of the biocrude [48, 49], which likely explains at least part of the increase in biocrude N recovery.

Another explanation is that the protein concentrations in slurries of Nan-1, Chl-1, Spi-1, and Mix-m are high enough to be in excess compared to carbohydrate concentrations for Maillard reactions, or, in other words, that carbohydrates could be the limiting reactant. In fact, Peterson et al. [31] found exactly that when examining hydrothermal degradation of glycine (an amino acid) and glucose (a sugar) alone and together; when glycine was in excess, increases in initial glucose concentration led to proportionally

greater glycine destruction. Such behavior in the present study would lead to a less-than-expected increase in the rate of N-cyclic formation from Maillard reactions due to increased protein content, allowing a greater proportion of the N in the protein to degrade to ammonium compared to the more protein-deficient and/or carbohydrate-rich biomass samples (Nan-2 and Chl-2). A third possibility is that the proportion of biomass N representing protein changes with increasing N-limitation (decreasing proteins and increasing lipids), which would obfuscate whether the changes in biocrude N recovery are due to protein or other, generally less abundant sources of N such as DNA and RNA. Regardless of the biochemical source, biocrude N recovery increases with decreasing biomass N content.

3.6. Sulfur content

3.6.1. Temperature, time, and slurry concentration

S content in the biocrude, depicted in Figure 5a, increases with increasing temperature and time until 300 °C and 3.2 min, at which point it plateaus (in the case of the higher-lipid species) or decreases, similar to the trends for N content and consistent with previous reports [12, 15, 17, 21]. There was no apparent global effect of initial concentration; however at 300 °C, 120 g L_{rxn}^{-1} slurries of Spi-1 (●), Chl-1 (■), and Chl-2 (■) on average produced biocrude with 0.10 wt% ($p < 0.03$) lower S content than the 30 g L_{rxn}^{-1} slurries, while those of Nan-1 (●) and Nan-2 (●) showed no effect or in some cases a slight increase for the 120 g L_{rxn}^{-1} slurries.

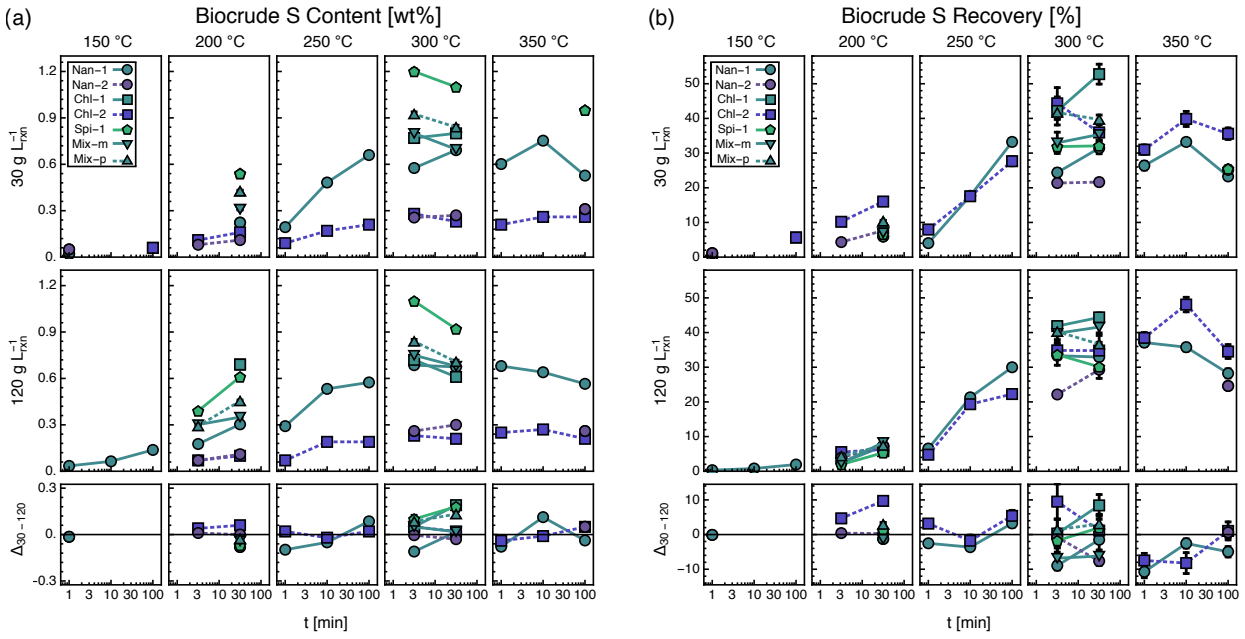

Figure 5: Biocrude sulfur (a) content and (b) recovery versus reaction time grouped by temperature and initial concentration. See Table 1 for microalgae types. The bottom row depicts the first row (30 g L_{rxn}^{-1}) minus the second row (120 g L_{rxn}^{-1}). Error bars indicate standard error.

3.6.2. Biochemical composition and species identity

Similar to N content, S content is a strong function of biochemical composition, with high-protein biomass producing biocrude with higher S content (color-coded in Fig. 5a; see Fig. B.5a in Appendix B for S content vs. protein content plots). Controlling for species identity, biocrude S content was on average 0.37 wt% ($p < 10^{-5}$) higher for higher-protein biomass than their lower-protein counterparts, an effect demonstrated previously [28]. The three feedstocks with similar biochemical composition, Nan-1 (●), Chl-1 (■), and Mix-m (▼), produced biocrude with significantly varied S content at low-to-moderate reaction severities, although at 300 °C, 31.6 min, these differences reduced to no more than 0.11 and 0.07 wt% for the 30 and 120 g L_{rxn}^{-1} slurries, respectively. This suggests that biochemical composition is a good predictor of biocrude S content at high reaction severity and that species identity is a significant factor at low severity only, which could be due to morphological differences between biomass types affecting the rate of S partitioning to the biocrude.

3.6.3. Two-species mixture interactions

At 200 °C, 31.6 min and higher reaction severities, measured (▼) S content was always lower than predicted (▲) in the two-species mixture by 0.10 wt% ($p < 0.002$) on average across those six different sets of conditions. It is not immediately clear why this would occur, but this effect was also previously observed by Madsen et al. [28] in various mixtures of biomass feedstocks, some of which similarly featured a high-protein feedstock paired with a high-carbohydrate feedstock. The trend points to reactions occurring in the bulk high-temperature water between compounds originating from both the high-protein *Spirulina* and high-lipid, high-carbohydrate *Chlorella* that inhibit some of the S from partitioning into the biocrude.

3.7. Sulfur recovery

S recovery in the biocrude usually increased with increasing temperature and time, shown in Figure 5b, similar to S content. However, on average S recovery did decrease by 8.8 % ($p < 0.03$) from 10 to 100 min at 350 °C for both initial concentrations of Nan-1 (●) and Chl-2 (■). There were no consistent global trends as a function of initial concentration, although certain types of biomass in particular showed consistent differences; for example, biocrude S recovery for the 30 g L_{rxn}^{-1} slurry of Chl-2 (■) was on average 8.0 % ($p < 0.05$) higher than the 120 g L_{rxn}^{-1} slurry for 300 °C, 3.2 min and milder reaction severities. In contrast to N recovery, there were also no globally consistent trends with respect to biochemical composition (Fig. B.5b); however, when controlling for species identity, there was an average increase in biocrude S recovery of 10 % ($p < 0.04$) as a function of increasing protein content across both initial concentrations at 300 °C and 31.6 min. The variability in biocrude S recovery due to species identity was at least 8.5 % and at most 21.3 % at 300 °C. This wide range in S recoveries suggests that more information, such as the abundance of specifically S-containing amino acids, is required to adequately predict S partitioning into the biocrude. The predicted

(▲) S recoveries for the two-species mixture matched the measured (▼) values for the 120 g L_{rxn}^{-1} across all conditions, but were predicted on average 5.5 % ($p < 0.09$) higher than measured for the 30 g L_{rxn}^{-1} slurry.

3.8. Oxygen content and recovery

3.8.1. Temperature and time

Biocrude O content ranged from 8.1 to 29.2 wt%, shown in Figure 6a. Starting at 200 °C, increasing reaction severity decreased biocrude O content, consistent with prior studies [12, 13, 15, 17, 21]. From 200 °C, 3.2 min to 300 °C, 31.6 min, for example, this reduction was on average about 10.6 wt% ($p < 10^{-6}$), a relative decrease of about 47 %. Notably, over this same range of conditions, the recovery of O in the biocrude (Fig. 6b) increases on average by 5.7 % ($p < 0.02$), indicating that there is actually a net influx of O into the biocrude over these conditions, but that the higher influx of other elements, primarily C and H, is diluting the overall O content. At higher reaction severities however, the average decrease in O content of 6.1 wt% ($p < 0.009$) is accompanied by a significant average reduction in O recovery of 7.3 % ($p < 0.03$), suggesting that deoxygenation is occurring.

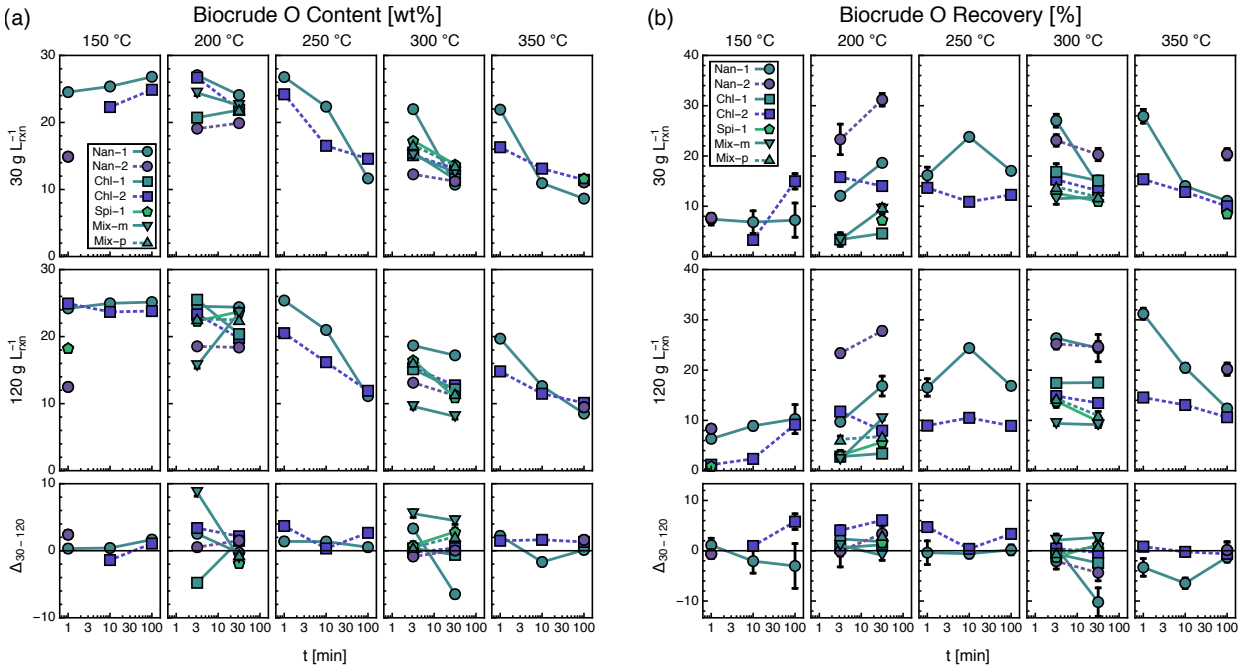

Figure 6: Biocrude oxygen (a) content and (b) recovery versus reaction time grouped by temperature and initial concentration. See Table 1 for microalgae types. The bottom row depicts the first row (30 g L_{rxn}^{-1}) minus the second row (120 g L_{rxn}^{-1}). Error bars indicate standard error.

3.8.2. Slurry concentration

There was no global effect of slurry concentration on O content, however there was a small, yet statistically significant average decrease in O recovery of 1.9 % ($p < 0.01$) with increasing slurry concentration at 200

°C for both reaction times. There is little information in the literature about the effect of concentration on biocrude O content, however Jazrawi et al. [21] found that increasing concentration (7 to 79 g L_{rxn}^{-1}) of a high-protein *Chlorella* slurry decreased biocrude O content at 300 and 350 °C for 3 min reaction time. In the present study, at 300 °C and 3.2 min, all four high-protein biomass types produced biocrude with on average 2.5 wt% ($p < 0.13$) lower O content with increasing initial concentration, which is comparable in magnitude to the study by Jazrawi et al. [21]. Jena et al. [12] also showed a slight decrease in biocrude O content from 64 to 144 g L_{rxn}^{-1} at 350 °C and 60 min holding time.

3.8.3. Biochemical composition and species identity

There similarly was no consistent overall trend in O content with respect to changing biochemical composition, although for specifically the two *Nannochloropsis* feedstocks, O content was on average 6.6 wt% higher ($p < 0.0002$) in the higher-protein strain, Nan-1 (●), than the lower-protein strain, Nan-2 (●), for reaction severities of 300 °C, 31.6 min and lower. Li et al. [26] showed a relatively weak trend of increasing biocrude O content with increasing biomass carbohydrate content, however the data from the present study did not show this trend (Fig. B.6a). Nan-1 (●), Chl-1 (■), and Mix-m (▼) produced biocrude with widely varying O content and recovery despite their similar biochemical profiles. After controlling for reaction conditions, the differences in O content and recovery ranged from 1.9 to 9.8 wt% and 3.3 to 17.0 %, respectively. These differences highlight the limit of proximate biochemical composition as a predictor for O partitioning in the biocrude.

3.8.4. Two-species mixture interactions

At 300 °C across both reaction times, the measured two-species mixture (▼) biocrude O contents and recoveries were on average 5.0 wt% higher ($p < 0.07$) and 2.4 % higher ($p < 0.08$), respectively, for the 30 g L_{rxn}^{-1} slurry compared to the 120 g L_{rxn}^{-1} slurry. Moreover, biocrude O contents for the 120 g L_{rxn}^{-1} slurry were actually lower than those of the component species with the lowest O content (i.e. Chl-2 (■) at 3.2 min and Spi-1 (●) at 31.6 min) by on average at least 4.3 wt%, and the same was true for O recovery, which was 2.6 % lower (absolute). These observations for a single initial concentration across two time points were not enough to demonstrate statistical significance, however at these conditions across both concentrations, the measured (▼) two-species mixture O contents and recoveries were lower than predicted (▲) by an average of 3.1 wt% ($p < 0.10$) and 2.3 wt% ($p < 0.11$), respectively. In other words, there was lower O content in the biocrude from the two-species mixture than expected at 300 °C (possibly even lower than any component species), and this effect is magnified by increasing initial concentration. This finding corroborates the results of Madsen et al. [28], which found that mixtures of high-protein and high-carbohydrate feedstocks led to decreased O content and increased N content in the biocrude oil. Increased N content was also observed in this study, discussed in Section 3.4. The reaction mechanism identified in that study, whereby nitrogen

degradation products shift reaction selectivities toward nitrogen-containing ring structures away from cyclic oxygenates, is therefore very likely to be occurring in the present study as well.

3.9. Phosphorus content and recovery

At a temperature of 300 °C and lower, biocrude P content and recovery, (Fig. B.7), stayed below 0.10 wt% and 2.3 %, respectively, for all samples measured; however, we note that these measurements were over a smaller subset of conditions than the other elemental analyses due to sample mass constraints. At 350 °C, some of the higher-lipid biomass samples produced biocrude with higher P content and recovery, although the highest observed were only 0.20 wt% and 8.3 %, respectively, in the case of Nan-2 (●) at 100 min, 30 g L_{rxn}^{-1}. These values were lower than reported by Valdez et al. [15] for similar experimental conditions but comparable to that of Jiang and Savage [50]. These data confirm that the majority of the phosphorus does not partition into the biocrude, especially at 300 °C and below; however, at 350 °C, a non-trivial amount of P (relative to the biomass P) may partition into the biocrude.

3.10. Higher-heating value

Biocrude HHV varied from 29.3 to 38.4 MJ kg^{-1} across all reaction conditions and feedstock characteristics, shown in Figure 7a. HHV increased monotonically with increasing reaction severity at 250 °C and higher for all biomass types, consistent with previous studies [12, 13, 15, 17]. There were no significant global trends in HHV with respect to initial concentration. Controlling for species identity and reaction conditions, biocrude HHV was on average 3.0 MJ kg^{-1} higher ($p < 0.00003$) for the higher-lipid strains compared to the lower-lipid strains, across all reaction conditions (color-coded in Fig. 7a; see Fig. B.8a in Appendix B for explicit HHV vs. lipid content plots). Even without controlling for species identity, biocrude HHV generally increased with increasing biomass lipid content, although at high reaction severities, the low-lipid Nan-1 (●) matched or exceed the HHV of the high-lipid Chl-2 (■). Li et al. [26] similarly found that biocrude HHV increased with increasing lipid content, but there was no clear association with protein content.

Biocrude HHV varied widely among Nan-1 (●), Chl-1 (■), and Mix-m (▼), although the average spread in values, across all reaction conditions, for the 30 g L_{rxn}^{-1} slurries (●/■/▼, ± 1.0 MJ kg^{-1}) was lower than that of the 120 g L_{rxn}^{-1} slurries (± 1.8 MJ kg^{-1}). At 300 °C across both reaction times, biocrude HHV for the two-species mixture was substantially higher for the 120 g L_{rxn}^{-1} slurry than the 30 g L_{rxn}^{-1} slurry, on average by about 2.3 MJ kg^{-1} ($p < 0.07$). Moreover, the HHV for the 120 g L_{rxn}^{-1} slurry of the two-species mixture was 0.6 MJ kg^{-1} higher ($p < 0.02$) than that of Chl-2 (■), the highest of the two component species, which follows a similar observation for O content in Section 3.8. These deviations from the expected values for HHV were largely due to significant increases in C content and decreases in O content.

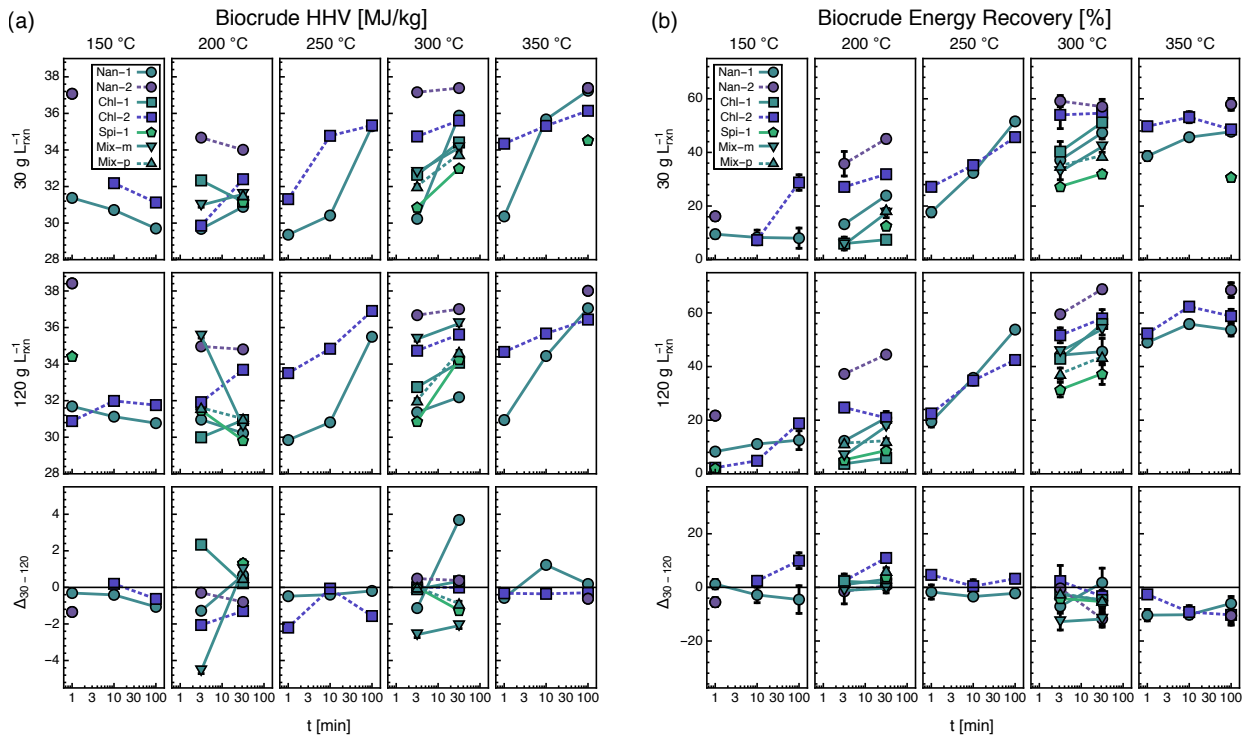

Figure 7: Biocrude (a) higher-heating value and (b) energy recovery versus reaction time grouped by temperature and initial concentration. See Table 1 for microalgae types. The bottom row depicts the first row (30 g L_{rxn}^{-1}) minus the second row (120 g L_{rxn}^{-1}). Error bars indicate standard error.

3.11. Energy recovery

Biocrude energy recovery, or the percentage of energy in the biocrude (biocrude HHV multiplied by yield) relative to the biomass HHV, followed the same general trends as biocrude yield (Figures 7b and B.8b). Notably, the higher-lipid 30 g L_{rxn}^{-1} slurries (●/■) reached a maximum energy recovery at just 300 °C and 3.2 min, while the higher-protein slurries (●/■/▼) continued to increase in energy recovery with increasing reaction severity. The 120 g L_{rxn}^{-1} slurries, however, exhibited largely the same trends with changing reaction severity, regardless of biochemical composition. For each biomass type at 300 °C and higher, the maximum energy recovery achievable was always higher for the 120 g L_{rxn}^{-1} slurries than their 30 g L_{rxn}^{-1} counterparts due to increased C recovery (Fig. B.2) and H recovery (Fig. B.3a), a trend that has been documented recently [22].

3.12. Mass balances, solid characteristics, and gas yield

The total mass balances, including the biocrude, solid, and aqueous fractions, are reported both without and with gas yields in Figures A.2a and b, respectively, in Appendix A. Mass closure was generally very good at 150 and 200 °C, but decreases with increasing reaction severity. We expect that a large portion of the lost

mass is comprised of volatile compounds in the aqueous phase. At high reaction severity (300 to 350 °C), some of the lost mass may be due to coke formation on the reactor walls as well. Data for solid yields and elemental content and recoveries are presented in Appendix C. Data for gas yields are presented in Appendix D. These data were not the primary focus of this study but we report them in the Appendices because they are important for quantifying the distribution of elements between the different phases produced during HTL.

3.13. Fatty-acid recovery

Figure 8 depicts saturated (SAFA), monounsaturated (MUFA), and polyunsaturated (PUFA) fatty-acid recoveries in the solid (green, bottom) and biocrude (brown, top) phases as functions of reaction temperature and time for the 120 g L_{rxn}^{-1} slurries of Nan-1 (●) and Chl-2 (■). As described in Section 2.4, these recoveries comprise fatty acids and their derivatives, such as fatty-acid amides, that retain the same chain structure and terminating carbonyl group. Plots for the 120 g L_{rxn}^{-1} slurries of other biomass types as well as data for the 30 g L_{rxn}^{-1} slurries are shown in Figures B.9 and C.8. Fatty-acid contents, recoveries, and class distributions in the biocrude and solids are shown in Tables B.5 through B.7 and C.5 through C.7, respectively.

3.13.1. Saturated fatty acids

SAFAs begin partitioning into the biocrude at conditions as mild as 150 °C and 10 min, and possibly even lower than that (there was insufficient biocrude generated by the 150 °C, 1 min reactions for analysis). In the case of the 120 g L_{rxn}^{-1} slurry of Nan-1 (●), SAFA recovery reaches a maximum of 93.8 wt% at 250 °C and 10 min (with similar recovery at comparable reaction severities), but then decreases with increasing reaction time. From 10 to 100 min at 350 °C, however, it actually increases back up to a recovery comparable to the maximum. In fact, when considering the 30 g L_{rxn}^{-1} slurries of Nan-1 and Chl-2 shown in Figure B.9a, SAFA recovery increased by on average 16.2 wt% ($p < 0.053$) from 10 to 100 min at 350 °C. Closer inspection reveals that this increase was partially due to an average absolute increase of 140 % ($p < 0.05$) in C18:0 recovery in the biocrude, shown in Figure B.10a and Table B.6, far more C18:0 than measured in the starting biomasses. Relative to all C18 fatty acids (including unsaturated), its recovery is still no greater than 12 wt%, shown in Figure B.10b. This suggests that unsaturated C18 fatty acids are hydrogenating to form C18:0 at 350 °C on the order of tens of minutes. This phenomenon has been suggested previously for similar HTL reaction conditions [51] due to the ability of high-temperature water to facilitate hydrogen production [6]. The extent of this hydrogenation of unsaturated C18 fatty acids to C18:0 increased with increasing slurry concentration as well, with C18:0 recovery increasing on average by about 78 % (absolute, $p < 0.02$). Notably, there was a large increase in C16:0 recovery at 350 °C, 100 min as well, but it was generally not enough to exceed 100 %, possibly because C16:0 is much more abundant in the original biomass.

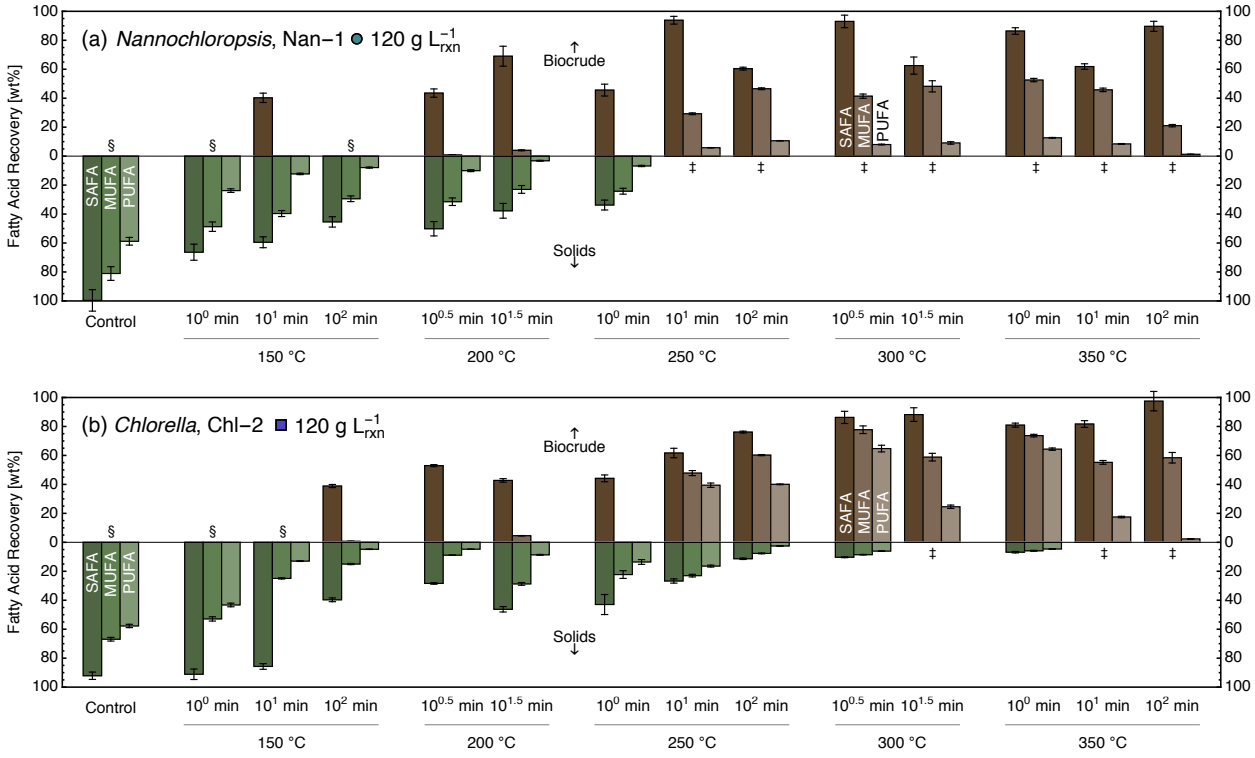

Figure 8: Saturated (SAFA), monounsaturated (MUFA), and polyunsaturated (PUFA) fatty-acid recoveries in the biocrude (brown, top) and solids (green, bottom) as functions of temperature and time for (a) low-lipid *Nannochloropsis* (Nan-1) and (b) high-lipid *Chlorella* (Chl-2). § and ‡ denote insufficient biocrude and solid mass for FAMEs analysis, respectively. Error bars indicate standard error.

3.13.2. Unsaturated fatty acids

In contrast, MUFAs and PUFAs in the biocrude were prevalent only at 250 °C, 10 min and higher reaction severities, significantly more severe than the mildest conditions for appreciable SAFA detection. Moreover, at mild reaction severities (below 250 °C, 10 min), these classes of fatty acids were not measured in either the solids or the biocrude phases; however, at higher reaction severities, there were appreciable amounts of both that exceeded their combined abundances in the solids and biocrude at mild reaction severity. There are two possible explanations for this phenomenon.

The first explanation is that MUFAs and PUFAs enjoy more stability in biocrude oil generated at reaction severities of at least 250 °C and 10 min than they do in the solid phase or in biocrude generated at milder temperatures. This hypothesis is supported by the reduction of MUFAs and PUFAs measured in the control experiments (left-most group of bars in Fig. 8), which were performed along with the actual reactions, but with no temperature treatment, and subsequently measured for fatty-acid content with the rest of the reaction products. This reduction highlights that some of the MUFAs and PUFAs degrade in the solids naturally over time, rather than purely through hydrothermal treatment. It is possible that this trend

holds for the biocrude perhaps as a function of the amount of other light-absorbing molecules in the oil which could protect the light-sensitive unsaturated fatty acids [52] from degrading as quickly. An additional explanation is that an intermediate reaction product is formed at mild conditions which reverts back to the original unsaturated fatty acid at moderate conditions. In authors' view, the former explanation is more likely than the latter, and further studies focusing on characterizing fatty-acid kinetics in high-temperature water would be needed to qualify the existence of an intermediate reaction product.

Notably, MUFA and PUFA recoveries were as high as 80.1 and 64.7 wt%, respectively, at 300 °C and 3.2 min for Nan-2 (●) and Chl-2 (■), shown in Figures B.9b and c, which includes Chl-2 in Fig. 8b. At this reaction condition, across both slurry concentrations for both the high-lipid Nan-2 and Chl-2, these recoveries were on average 76.4 and 53.3 wt% for MUFAs and PUFAs, respectively. To the authors' knowledge, no study of microalgal HTL has demonstrated such high recovery of both mono- and polyunsaturated fatty acids in the biocrude at those conditions.

Several recent studies reported MUFA and PUFA recovery in the biocrude at temperatures in the range of 225 to 240 °C and 20 to 30 min holding time (not including heat up), but they were not reported in excess of 35 wt% [53, 54]. Another showed appreciable MUFA (14.1 wt%) and PUFA (20.7 wt%) content in the biocrude produced from a high-lipid *Chlorella* at 260 °C, 60 min holding time which was comparable to that at similar conditions presented herein [49]; however, initial biomass MUFA and PUFA content were not provided for determination of recovery. Several other studies conducted at higher reaction severity, including 300 °C (or higher) and at least 30 min total reaction time (including heat up), observed MUFA and PUFA recoveries of up to 85 and 9 wt%, respectively [25, 55, 56]. The MUFA recoveries reported therein are comparable to those presented here, but the reported PUFA recoveries were all significantly lower. These lower PUFA recoveries are likely the result of longer total reaction times employed in these studies, either by design or necessity due to longer heat up times, given that the PUFA recoveries in the present study at 300 °C and 31.6 min are substantially lower than at 3.2 min.

The data show that high PUFA recoveries are only achievable with higher-lipid microalgae. These findings suggest that fast HTL (300 °C and 3.2 min total reaction time) is an effective method for extracting all types of fatty acids without significantly degrading their structure, especially for high-lipid microalgae. Preserving the structure of the unsaturated fatty acids is of particular interest for downstream upgrading (more double bonds allows for more types of upgrading chemistries) as well for sale as high-value nutraceutical compounds, particularly omega-3 PUFAs [57].

At reaction times longer than 3.2 and 1 min at temperatures of 300 °C and 350°C, respectively, MUFA recovery generally decreased and PUFA recovery monotonically decreased for all biomass types and concentrations (Fig. 8 and B.9). Fatty acids exhibit lower hydrothermal stability with increasing degrees of unsaturation, due to the increase in reactivity afforded by the additional double bonds [58]. Johnson and Tester [59] calculated kinetic parameters for triglyceride hydrolysis and subsequent unsaturated-fatty-

acid degradation at comparable HTL conditions; they proposed that the timescale for degradation suggests reaction times of 30 min or less at temperature of 300 to 350 °C are optimal for maximizing unsaturated-fatty-acid yields. In the present study, reaction severities above the range of 300 °C, 3.2 min and 350 °C, 1 min resulted in lower MUFA and especially lower PUFA recoveries in the biocrude. This suggests that the timescale for unsaturated-fatty-acid degradation is actually on the order of just minutes, much shorter than proposed by Johnson and Tester [59] and a novel finding arising from the use of reactors that fully heat up in just 1 min.

3.13.3. Total fatty acids

Total fatty-acid recovery, depicted in Figure B.9d, followed the same trends with respect to temperature and time reported above for all biomass types, and was not globally affected by initial concentration. It did however increase on average by 26.2 wt% ($p < 10^{-5}$) with increasing lipid content, across all reaction conditions after controlling for species identity. This trend was true for each class of fatty acid as well, with an increase of 8.1 wt% ($p < 0.04$), 28.5 wt% ($p < 0.0004$), and 14.0 wt% ($p < 0.007$) for SAFA, MUFA, and PUFA recoveries, respectively. Those trends highlight that not only do higher-lipid biomass samples produce biocrude oil with higher fatty-acid content, but actually recover higher percentages of all classes of fatty acids than their higher-protein counterparts. This could be due to an increased prevalence of side reactions between protein degradation products and the fatty acids in the high-protein strains. The higher magnitudes of increases for MUFA and PUFA recoveries suggests it could be due to the inhibition of side reactions with the double bonds, likely in addition to reactions with the carboxyl group.

4. Further discussion and conclusion

Table 2 presents a summary of the impacts of changing reaction time, slurry concentration, lipid content, protein content, species, and reaction temperature on the yield and properties of the biocrude oil. These changes control for all other factors and occur from two reference points at 200 and 300 °C, respectively, for 30 g L_{rxn}^{-1} slurries and 3.2 min reaction time.

4.1. Mild-reaction-severity reference point

At the 200 °C, 3.2 min, and 30 g L_{rxn}^{-1} reference point, biocrude properties are most sensitive to changing lipid content and temperature. In fact, an average increase from 10.5 to 24.2 wt% lipid content resulted in very similar increases in biocrude yield, C recovery, and energy recovery as did an increase in temperature from 200 to 300 °C, all of which were statistically significant. Linear approximation reveals that a 1 wt% increase in lipid content produces an equivalent increase in biocrude C recovery (+1.5 %) as does a 5.8 °C increase in reaction temperature. Notably however, increasing temperature also resulted in statistically

Ref. Point	Independent Variable	Change	Sensitivity Scale	Yield	Content [wt%]					HHV	Recovery [%]									
				[wt%]	C	H	N	S	O	[kJ/g]	C	H	N	S	O	ER	SA	MU	PU	TF
200 °C 3.2 min 30 g L_{rxn}^{-1}	Temperature:	200 → 300 °C		18*	4	−0.2	3.1*	0.2*	−8*	2	26*	22*	17*	26	7	27*	11	37	26	26
	Lipid Content:	10.5 → 24.2 wt%		16*	1	0.7	−0.7	−[a]	−1	1	21*	21	3	−	12*	22*	−	−	−	−
	Protein Content:	17.4 → 42.6 wt%		−16*	−1	−0.7	0.7	−	1	−1	−21*	−21	−3	−	−12*	−22*	−	−	−	−
	Species:	Nan−1, Chl−1, Mix−m		4	3	0.1	0.4	−	3	1	4	5	0	−	5	4	−	−	−	−
	Time:	3.2 → 31.6 min		6*	1	0.1	0.7*	0.0	−2	1	7*	7*	2*	3	4	8*	5	5	0	4
	Concentration:	30 → 120 g L_{rxn}^{-1}		0	1	0.4	0.2	0.0	−2	1	−1	−1	0	−2	−2	−1	−2	−1	0	−1
300 °C 3.2 min 30 g L_{rxn}^{-1}	Lipid Content:	10.5 → 24.2 wt%		10	7	1.3	−2.8	−0.4	−5	5	16	15	8*	0	−3	18	−4	61	52	46
	Protein Content:	17.4 → 42.6 wt%		−10	−7	−1.3	2.8	0.4	5	−5	−16	−15	−8*	0	3	−18	4	−61	−52	−46
	Species:	Nan−1, Chl−1, Mix−m		5	3	0.1	0.9	0.1	4	1	4	4	2	9	8	4	21	30	21	18
	Time:	3.2 → 31.6 min		2	4*	0.3	0.1	0.0	−4*	2	5	4	3*	2	−3	6	−8	−9	−22	−12
	Concentration:	30 → 120 g L_{rxn}^{-1}		2	1	0.1	0.6*	0.0	−1	1	4	3	3*	1	0	4	2	6	9	7

Table 2: Summary of differences in biocrude properties as a result of changing six different independent variables from two different reference points. Sensitivity Scale qualitatively denotes the sensitivity of biocrude properties to each independent variable at a given reference point. ER represents energy recovery [%]. SA, MU, PU, and TF are saturated, monounsaturated, polyunsaturated, and total fatty-acid recovery in the biocrude, respectively. Yellow and blue intensity denote increases and decreases in the associated property, respectively. Changes in temperature, time, and concentration are the average of the differences in the six different types of biomass (see Table 1). Changes in biochemical composition show the average of differences in the two different types of *Nannochloropsis* and *Chlorella*, respectively. Changes in species denote the standard deviation of values from Nan-1, Chl-1, and Mix-m. [a]Denotes no data available. *Denotes statistically significant difference at the 0.05 level.

significant increases in N content (+3.1 wt%) and N recovery (+17 %) in the biocrude whereas increasing lipid content decreased N content (-0.7 wt%) and slightly increased N recovery (+3 %).

The effect of increasing protein content was (necessarily) of equal magnitude but opposite sign of that of increasing lipid content, but over about twice as wide of a range in protein content (25.2 wt%) than lipid content (13.7 wt%). In general, increasing protein content negatively affected the yield and composition of the biocrude oil at this reference point, however it did decrease both N (-3%) and O (-12%) recovery. The variabilities in biocrude properties induced by different microalgae species were similar in magnitude to the effects of increasing reaction time from 3.1 to 31.6 min. Finally, a four-fold increase in concentration at this reference point did not affect biocrude properties to a significant extent.

4.2. High-reaction-severity reference point

At the 300 °C, 3.2 min, and 30 g L_{rxn}^{-1} reference point, the characteristics of the biocrude are most sensitive to changing biochemical composition. Increased lipid content produced similar trends in biocrude properties as at 200 °C; however, the increases to yield, C content and recovery, H content and recovery, and energy recovery were lower, and the decreases to N and O content were higher. Increased protein content was again detrimental to the yield and composition of the biocrude, although it decreased N recovery (-8%) to a statistically significant extent, greater than that at 200 °C.

Species identity, reaction time, and slurry concentration demonstrated around the same magnitude of effects on biocrude yield and properties. Increased time and concentration both induced similar changes in

biocrude yield and elemental content and recovery; although, increased time substantially reduced fatty-acid recovery while increased concentration slightly increased it.

4.3. Significance of results in algal biofuel production

The viability of renewable fuel production from microalgae via hydrothermal liquefaction (HTL) hinges on the minimization of energy and material inputs and costs required for four major process units: (A) algal cultivation and (B) dewatering, (C) HTL, and (D) catalytic upgrading. We present hypothetical, yet reasonable, strategies for operating these process units using either a low- or a high-input strategy in Table 3, where "input" refers to the amalgamation of energy, materials, and costs. These strategies either minimize the inputs for a process unit locally (assuming that this unit has high input requirements relative to the total process inputs) or employ relatively more inputs locally to reduce inputs for other process units, and thus the process overall (assuming that this unit has lower input requirements relative to the total process inputs.) An approach often described in the field is to (A) maximize biomass productivity while minimizing inputs (generating high-protein biomass [60]) and (B) concentrate to high levels (e.g., 16 wt%) to reduce energy spent heating water during (C) HTL at high reaction severity to maximize biocrude yield. This biocrude is typically $>$ 5 wt% in N content due to the high-protein biomass and severe reaction conditions and must be (D) upgraded to lower levels ($<$ 0.5 wt%) before conventional refining [61]. This collective approach minimizes inputs for Step A (on a per-unit-biomass basis) above all else. Parameters for Steps B and C are chosen to maximize biocrude yield and the inputs required to remove heteroatoms in Step D are generally assumed to be relatively small.

Step	Process unit	Low-input strategy	High-input strategy
A	Algal growth	Maximize biomass (high-protein content)	Maximize lipid content (less biomass)
B	Dewatering	Concentrate by 200 to 800x to 4 wt%	Concentrate by 800 to 3200x to 16 wt%
C	Hydrothermal liquefaction	Mild reaction severity (e.g. 200 °C, 31.6 min)	High reaction severity (e.g. 350 °C, 100 min)
D	Catalytic upgrading	Upgrade from <3 wt% N content	Upgrade from >5 wt% N content

Table 3: Examples for strategies to either minimize process unit inputs locally (low-input strategy; assuming large or many input requirements relative to total process inputs) or employ relatively more inputs locally to reduce inputs of other process units (high-input strategy; assuming small or few input requirements relative to total process inputs). Values chosen represent reasonable examples but are not comprehensive.

The work herein provides empirical, quantitative evidence of some of the effects that this approach has on biocrude yield and properties. Moreover this study allows quantitative comparison for other competing strategies. The results of this study show that both higher protein content (resulting from low-input growth strategy for Step A) and higher concentration (resulting from biocrude yield-maximizing strategy for Step B) independently lead to higher biocrude N content at nearly all reaction severities (Step C), with the exception of 350 °C and 100 min. At 300 °C, these effects are +2.8 wt% and +0.6 wt%, respectively, for a total of

+3.4 wt% N content, all of which must be removed via Step D to produce a viable fuel. N can be a difficult heteroatom to remove [62] and is often incorporated in heterocyclic saturated or aromatic compounds [28] which themselves are difficult to refine into more useful compounds without expending a relatively large amount of energy.

An alternative strategy is to maximize biomass lipid content, which decreases biomass productivity and protein content and takes more time to grow (Step A) compared to high-protein biomass [25, 60]. On a per-unit-biomass basis, this approach would require more raceway ponds to compensate for lost productivity, therefore requiring more inputs than the previous strategy. However, when high-lipid biomass is reacted at lower concentration (Step B), it produces biocrude (Step C) with 3.4 wt% less N content than protein-rich biomass at high concentration. In this scenario, biocrude yield is also 8 wt% higher (net), contains higher C and H content and less S and O content, leading to overall improved energy density. These shifts in elemental contents benefit the ease of upgrading the biocrude (Step D) to a more reasonable petroleum substitute, given that the starting contents of heteroatoms are far lower. Additionally, overall C and H recovery are 11 and 12 % higher (net) on average as well, and unsaturated and total fatty-acid recoveries are both around 50 % higher compared to that of the highly concentrated high-protein slurries, indicating that a greater abundance of higher-quality hydrocarbons reside in the biocrude.

In summary, this work further characterizes the HTL process unit, and how upstream parameters (algal growth and dewatering) can impact downstream parameters (catalytic upgrading) that ultimately control the economic feasibility and environmental sustainability of biofuel production via microalgal biorefining. Optimizing approaches (i.e. maximizing productivity vs. lipid content) for the production of biocrude oil from microalgae via HTL lie primarily with assumptions regarding algal growth and catalytic upgrading; for example, the additional inputs required to cultivate high-lipid biomass to reduce inputs for catalytic upgrading must be quantitatively compared with the fewer inputs required to grow high-protein biomass but with significantly more inputs required for catalytic upgrading. The results herein suggest that modest reductions in biomass productivity in favor of enhanced lipid content could be more than offset by decreases in biocrude heteroatom content and increased energy density. In more practical terms, this means that high-lipid microalgae may have a greater likelihood of producing high-quality biofuel with higher energy return on investment. Additional work is needed to quantify and characterize the catalytic upgrading process, which has received far less attention than HTL, but must be well-understood for comprehensive process optimization.

4.4. Additional conclusions

In addition to the aforementioned effects, there were several other key takeaways from this study. Maillard reactions explained some observed increases in biocrude yield, C recovery, and N recovery and associated decreases in O recovery. Moreover, the selectivities of these reactions were promoted by increases in concen-

tration, as evidenced by the differences between the measured and observed values for a two-species mixture of a high-protein biomass (Spi-1) and a high-carbohydrate biomass (Chl-2). Furthermore, carbohydrates may act as the limiting reactant in an excess of protein for these reactions, causing a greater proportion of N recovery in the biocrude for biomass samples with higher carbohydrate-to-protein ratios (e.g., Chl-2 and Nan-1). Additionally, we found that fast HTL (300 °C, 3.2 min) of more dilute slurries of high-lipid biomass is an effective method for recovering up to 89.3, 80.1, and 64.7 wt% of saturated, monounsaturated, and polyunsaturated fatty acids, respectively. These results together suggest that high-lipid and low-carbohydrate biomass may be optimal for producing high-quality biocrude and limiting the extent of Maillard reactions, although future work is needed to optimize the relative proportions of proteins and carbohydrates for the minimization of Maillard reactions during HTL.

Acknowledgements

We thank Catherine Griffith for assistance with FAME analysis. The U.S. National Science Foundation provided financial support via a grant from the Emerging Frontiers in Research Innovation (award no. 1332342). The Rackham Predoctoral Fellowship from the University of Michigan also provided financial support.

Conflicts of Interest

The authors declare no conflict of interest.

Appendices A-D. Supplementary material

Appendix A presents additional details pertaining to experimental methods, including biomass elemental and fatty-acid contents. Appendix B presents tabular data for biocrude yield, elemental composition and recoveries, and fatty-acid content, recovery, and distribution. Appendix B also contains supplemental figures for these biocrude properties with respect to time or biochemical content. Appendix C presents tabular data for solid yield, elemental composition and recoveries, and fatty-acid content, recovery, and distribution. Appendix C also contains supplemental figures for these solid properties with respect to time or biochemical content. Appendix D contains a table and figure of gas yields. Supplementary data associated with this article can be found in the online version.

References

[1] Y. Chisti, Biodiesel from microalgae, Biotechnology advances 25 (3) (2007) 294–306, doi:10.1016/j.biotechadv.2007.02.001.

[2] L. Brennan, P. Owende, Biofuels from microalgae-A review of technologies for production, processing, and extractions of biofuels and co-products, Renewable and Sustainable Energy Reviews 14 (2) (2010) 557–577, doi:10.1016/j.rser.2009.10.009.

[3] P. T. Pienkos, A. Darzins, The promise and challenges of microalgal-derived biofuels, Biofuels, Bioproducts and Biorefining 3 (4) (2009) 431–440, doi:10.1002/bbb.159.

[4] A. Bhatnagar, S. Chinnasamy, M. Singh, K. C. Das, Renewable biomass production by mixotrophic algae in the presence of various carbon sources and wastewaters, Applied Energy 88 (10) (2011) 3425–3431, doi:10.1016/j.apenergy.2010.12.064.

[5] S. M. Heilmann, H. T. Davis, L. R. Jader, P. A. Lefebvre, M. J. Sadowsky, F. J. Schendel, M. G. von Keitz, K. J. Valentas, Hydrothermal carbonization of microalgae, Biomass and Bioenergy 34 (6) (2010) 875–882, doi:10.1016/j.biombioe.2010.01.032.

[6] N. Akiya, P. E. Savage, Roles of water for chemical reactions in high-temperature water., Chemical reviews 102 (8) (2002) 2725–2750.

[7] S. M. Changi, J. L. Faeth, N. Mo, P. E. Savage, Hydrothermal Reactions of Biomolecules Relevant for Microalgae Liquefaction, Industrial & Engineering Chemistry Research 54 (47) (2015) 11733–11758, doi:10.1021/acs.iecr.5b02771.

[8] P. Duan, P. E. Savage, Catalytic hydrotreatment of crude algal bio-oil in supercritical water, Applied Catalysis B: Environmental 104 (1-2) (2011) 136–143, doi:10.1016/j.apcatb.2011.02.020.

[9] D. C. Elliott, T. R. Hart, A. J. Schmidt, G. G. Neuenschwander, L. J. Rotness, M. V. Olarte, A. H. Zacher, K. O. Albrecht, R. T. Hallen, J. E. Holladay, Process development for hydrothermal liquefaction of algae feedstocks in a continuous-flow reactor, Algal Research 2 (4) (2013) 445–454, doi:10.1016/j.algal.2013.08.005.

[10] J. M. Jarvis, K. O. Albrecht, J. M. Billing, A. J. Schmidt, R. T. Hallen, T. M. Schaub, Assessment of Hydrotreatment for Hydrothermal Liquefaction Biocrudes from Sewage Sludge, Microalgae, and Pine Feedstocks, Energy and Fuels 32 (2018) 8483–8493, doi:10.1021/acs.energyfuels.8b01445.

[11] D. Chiaramonti, M. Prussi, M. Buffi, A. M. Rizzo, L. Pari, Review and experimental study on pyrolysis and hydrothermal liquefaction of microalgae for biofuel production, Applied Energy 185 (2017) 963–972, doi:10.1016/j.apenergy.2015.12.001.

[12] U. Jena, K. C. Das, J. R. Kastner, Effect of operating conditions of thermochemical liquefaction on biocrude production from Spirulina platensis, Bioresource Technology 102 (10) (2011) 6221–6229, doi:10.1016/j.biortech.2011.02.057.

[13] L. Garcia Alba, C. Torri, C. Samorì, J. Van Der Spek, D. Fabbri, S. R. A. Kersten, D. W. F. W. Brilman, Hydrothermal Treatment (HTT) of Microalgae: Evaluation of the Process As Conversion Method in an Algae Biorefinery Concept, Energy & Fuels 26 (1) (2012) 642–657, doi:10.1021/ef201415s.

[14] C. Miao, M. Chakraborty, S. Chen, Impact of reaction conditions on the simultaneous production of polysaccharides and bio-oil from heterotrophically grown Chlorella sorokiniana by a unique sequential hydrothermal liquefaction process, Bioresource Technology 110 (2012) 617–627, doi:10.1016/j.biortech.2012.01.047.

[15] P. J. Valdez, M. C. Nelson, H. Y. Wang, X. N. Lin, P. E. Savage, Hydrothermal liquefaction of Nannochloropsis sp.: Systematic study of process variables and analysis of the product fractions, Biomass and Bioenergy 46 (2012) 317–331, doi:10.1016/j.biombioe.2012.08.009.

[16] J. L. Faeth, P. J. Valdez, P. E. Savage, Fast Hydrothermal Liquefaction of Nannochloropsis sp. To Produce Biocrude, Energy & Fuels 27 (3) (2013) 1391–1398, doi:10.1021/ef301925d.

[17] P. S. Christensen, G. G. Peng, F. Vogel, B. B. Iversen, Hydrothermal Liquefaction of the Microalgae Phaeodactylum tricornutum : Impact of Reaction Conditions on Product and Elemental Distribution, Energy & Fuels 28 (9) (2014) 5792–5803, doi:10.1021/ef5012808.

[18] P. J. Valdez, V. J. Tocco, P. E. Savage, A general kinetic model for the hydrothermal liquefaction of microalgae, Bioresource Technology 163 (2014) 123–127, doi:10.1016/j.biortech.2014.04.013.

[19] D. C. Hietala, J. L. Faeth, P. E. Savage, A quantitative kinetic model for the fast and isothermal hydrothermal liquefaction

of Nannochloropsis sp., Bioresource Technology 214 (2016) 102–111, doi:10.1016/j.biortech.2016.04.067.

[20] J. H. Yang, H. Y. Shin, Y. J. Ryu, C. G. Lee, Hydrothermal liquefaction of Chlorella vulgaris: Effect of reaction temperature and time on energy recovery and nutrient recovery, Journal of Industrial and Engineering Chemistry doi: 10.1016/j.jiec.2018.07.053.

[21] C. Jazrawi, P. Biller, A. B. Ross, A. Montoya, T. Maschmeyer, B. S. Haynes, Pilot plant testing of continuous hydrothermal liquefaction of microalgae, Algal Research 2 (3) (2013) 268–277, doi:10.1016/j.algal.2013.04.006.

[22] W.-T. Chen, W. Qian, Y. Zhang, Z. Mazur, C.-T. Kuo, K. Scheppe, L. C. Schideman, B. K. Sharma, Effect of ash on hydrothermal liquefaction of high-ash content algal biomass, Algal Research 25 (2017) 297–306, doi: 10.1016/j.algal.2017.05.010.

[23] P. Biller, A. B. Ross, Potential yields and properties of oil from the hydrothermal liquefaction of microalgae with different biochemical content., Bioresource Technology 102 (1) (2011) 215–225, doi:10.1016/j.biortech.2010.06.028.

[24] D. López Barreiro, C. Zamalloa, N. Boon, W. Vyverman, F. Ronsse, W. Brilman, W. Prins, Influence of strain-specific parameters on hydrothermal liquefaction of microalgae., Bioresource Technology 146 (2013) 463–471, doi: 10.1016/j.biortech.2013.07.123.

[25] S. Leow, J. R. Witter, D. R. Vardon, B. K. Sharma, J. S. Guest, T. J. Strathmann, Prediction of microalgae hydrothermal liquefaction products from feedstock biochemical composition, Green Chem. 17 (6) (2015) 3584–3599, doi: 10.1039/C5GC00574D.

[26] Y. Li, S. Leow, A. C. Fedders, B. K. Sharma, J. S. Guest, T. J. Strathmann, Quantitative multiphase model for hydrothermal liquefaction of algal biomass, Green Chem. 19 (4) (2017) 1163–1174, doi:10.1039/C6GC03294J.

[27] D. C. Hietala, C. K. Koss, A. Narwani, A. R. Lashaway, C. M. Godwin, B. J. Cardinale, P. E. Savage, Influence of biodiversity, biochemical composition, and species identity on the quality of biomass and biocrude oil produced via hydrothermal liquefaction, Algal Research 26 (May) (2017) 203–214, doi:10.1016/j.algal.2017.07.020.

[28] R. B. Madsen, R. Z. K. Bernberg, P. Biller, J. Becker, B. B. Iversen, M. Glasius, Hydrothermal co-liquefaction of biomasses quantitative analysis of bio-crude and aqueous phase composition, Sustainable Energy Fuels 1 (4) (2017) 789–805, doi: 10.1039/C7SE00104E.

[29] R. Shakya, S. Adhikari, R. Mahadevan, S. R. Shanmugam, H. Nam, E. B. Hassan, T. A. Dempster, Influence of biochemical composition during hydrothermal liquefaction of algae on product yields and fuel properties, Bioresource Technology 243 (2017) 1112–1120, doi:10.1016/j.biortech.2017.07.046.

[30] R. B. Madsen, P. Biller, M. M. Jensen, J. Becker, B. B. Iversen, M. Glasius, Predicting the chemical composition of aqueous phase from hydrothermal liquefaction of model compounds and biomasses, Energy & Fuels doi: 10.1021/acs.energyfuels.6b02007.

[31] A. A. Peterson, R. P. Lachance, J. W. Tester, Kinetic evidence of the maillard reaction in hydrothermal biomass processing: Glucose-glycine interactions in high-temperature, high-pressure water, Industrial and Engineering Chemistry Research 49 (5) (2010) 2107–2117, doi:10.1021/ie9014809.

[32] J. L. Faeth, P. E. Savage, J. M. Jarvis, A. M. McKenna, P. E. Savage, Characterization of products from fast and isothermal hydrothermal liquefaction of microalgae, AIChE Journal 62 (3) (2016) 815–828, doi:10.1002/aic.15147.

[33] R. B. Levine, A. A. Bollas, M. D. Durham, P. E. Savage, Triflate-catalyzed (trans)esterification of lipids within carbonized algal biomass, Bioresource Technology 111 (2012) 222–229, doi:10.1016/j.biortech.2012.02.055.

[34] APHA, Standard Methods for the Examination of Water and Wastewater: Including Bottom Sediments and Sludges, American Public Health Association, New York, 1995.

[35] C. M. Godwin, D. C. Hietala, A. R. Lashaway, A. Narwani, P. E. Savage, B. J. Cardinale, Ecological Stoichiometry Meets Ecological Engineering: Using Polycultures to Enhance the Multifunctionality of Algal Biocrude Systems, Environmental Science & Technology 51 (19) (2017) 11450–11458, doi:10.1021/acs.est.7b02137.

[36] B. J. Bellinger, B. A. Van Mooy, J. B. Cotner, H. F. Fredricks, C. R. Benitez-Nelson, J. Thompson, A. Cotter, M. L. Knuth, C. M. Godwin, Physiological modifications of seston in response to physicochemical gradients within Lake Superior, Limnology and Oceanography 59 (3) (2014) 1011–1026, doi:10.4319/lo.2014.59.3.1011.

[37] S. A. Channiwala, P. P. Parikh, A unified correlation for estimating HHV of solid, liquid and gaseous fuels, Fuel 81 (8) (2002) 1051–1063, doi:10.1016/S0016-2361(01)00131-4.

[38] S. O. Lourenço, E. Barbarino, P. L. Lavín, U. M. Lanfer Marquez, E. Aidar, Distribution of intracellular nitrogen in marine microalgae: Calculation of new nitrogen-to-protein conversion factors, European Journal of Phycology 39 (1) (2004) 17–32, doi:10.1080/0967026032000157156.

[39] S. Guo, X. Dong, C. Zhu, Y. Han, Z. Wang, A simple modeling approach for characteristics analysis of hydrothermal liquefaction products from low-lipid aquatic plants, Applied Thermal Engineering 125 (2017) 394–400, doi:10.1016/j.applthermaleng.2017.07.042.

[40] G. Teri, L. Luo, P. E. Savage, Hydrothermal Treatment of Protein, Polysaccharide, and Lipids Alone and in Mixtures, Energy & Fuels 28 (12) (2014) 7501–7509, doi:10.1021/ef501760d.

[41] J. M. Jarvis, J. M. Billing, Y. E. Corilo, A. J. Schmidt, R. T. Hallen, T. M. Schaub, FT-ICR MS analysis of blended pine-microalgae feedstock HTL biocrudes, Fuel 216 (December 2017) (2018) 341–348, doi:10.1016/j.fuel.2017.12.016.

[42] J. Yang, Q. S. He, K. Corscadden, H. Niu, The impact of downstream processing methods on the yield and physiochemical properties of hydrothermal liquefaction bio-oil, Fuel Processing Technology 178 (2018) 353–361, doi:10.1016/j.fuproc.2018.07.006.

[43] J. Yang, Q. S. He, H. Niu, K. Corscadden, T. Astatkie, Hydrothermal liquefaction of biomass model components for product yield prediction and reaction pathways exploration, Applied Energy 228 (2018) 1618–1628, doi:10.1016/j.apenergy.2018.06.142.

[44] A. Kruse, A. Krupka, V. Schwarzkopf, C. Gamard, T. Henningsen, Influence of Proteins on the Hydrothermal Gasification and Liquefaction of Biomass. 1. Comparison of Different Feedstocks, Industrial & Engineering Chemistry Research 44 (9) (2005) 3013–3020, doi:10.1021/ie049129y.

[45] A. Croce, E. Battistel, S. Chiaberge, S. Spera, F. De Angelis, S. Reale, A Model Study to Unravel the Complexity of Bio-Oil from Organic Wastes, ChemSusChem 10 (1) (2017) 171–181, doi:10.1002/cssc.201601258.

[46] B. E. Eboibi, D. M. Lewis, P. J. Ashman, S. Chinnasamy, Effect of operating conditions on yield and quality of biocrude during hydrothermal liquefaction of halophytic microalga Tetraselmis sp., Bioresource Technology 170 (2014) 20–29, doi:10.1016/j.biortech.2014.07.083.

[47] W. T. Chen, Y. Zhang, J. Zhang, G. Yu, L. C. Schideman, P. Zhang, M. Minarick, Hydrothermal liquefaction of mixed-culture algal biomass from wastewater treatment system into bio-crude oil, Bioresource Technology 152 (2014) 130–139, doi:10.1016/j.biortech.2013.10.111.

[48] W.-T. Chen, Y. Zhang, J. Zhang, L. Schideman, G. Yu, P. Zhang, M. Minarick, Co-liquefaction of swine manure and mixed-culture algal biomass from a wastewater treatment system to produce bio-crude oil, Applied Energy 128 (2014) 209–216, doi:10.1016/j.apenergy.2014.04.068.

[49] O. Palardy, C. Behnke, L. M. L. Laurens, Fatty Amide Determination in Neutral Molecular Fractions of Green Crude Hydrothermal Liquefaction Oils From Algal Biomass, Energy & Fuels 31 (8) (2017) 8275–8282, doi:10.1021/acs.energyfuels.7b01175.

[50] J. Jiang, P. E. Savage, Metals and Other Elements in Biocrude from Fast and Isothermal Hydrothermal Liquefaction of Microalgae, Energy & Fuels (2017) acs.energyfuels.7b03144doi:10.1021/acs.energyfuels.7b03144.

[51] P. Biller, R. Riley, A. B. Ross, Catalytic hydrothermal processing of microalgae: decomposition and upgrading of lipids., Bioresource Technology 102 (7) (2011) 4841–4848, doi:10.1016/j.biortech.2010.12.113.

[52] A. Ottolenghi, F. Bernheim, K. M. Wilbur, The inhibition of certain mitochondrial enzymes by fatty acids oxidized

by ultraviolet light or ascorbic acid, Archives of Biochemistry and Biophysics 56 (1) (1955) 157–164, doi:10.1016/0003-9861(55)90345-3.

[53] H. K. Reddy, T. Muppaneni, S. Ponnusamy, N. Sudasinghe, A. Pegallapati, T. Selvaratnam, M. Seger, B. Dungan, N. Nirmalakhandan, T. Schaub, F. O. Holguin, P. Lammers, W. Voorhies, S. Deng, Temperature effect on hydrothermal liquefaction of Nannochloropsis gaditana and Chlorella sp., Applied Energy 165 (2016) 943–951, doi:10.1016/j.apenergy.2015.11.067.

[54] J. S. Martinez-Fernandez, S. Chen, Sequential Hydrothermal Liquefaction characterization and nutrient recovery assessment, Algal Research 25 (May) (2017) 274–284, doi:10.1016/j.algal.2017.05.022.

[55] C. Miao, M. Chakraborty, T. Dong, X. Yu, Z. Chi, S. Chen, Sequential hydrothermal fractionation of yeast Cryptococcus curvatus biomass., Bioresource technology 164 (2014) 106–12, doi:10.1016/j.biortech.2014.04.059.

[56] F. Cheng, Z. Cui, L. Chen, J. Jarvis, N. Paz, T. Schaub, N. Nirmalakhandan, C. E. Brewer, Hydrothermal liquefaction of high- and low-lipid algae: Bio-crude oil chemistry, Applied Energy 206 (August) (2017) 278–292, doi:10.1016/j.apenergy.2017.08.105.

[57] DOE (U.S. Department of Energy), National Algal Biofuels Technology Review, Tech. Rep., U.S. Department of Energy, Office of Energy Efficiency and Renewable Energy, Bioenergy Technologies Office, 2016.

[58] H.-Y. Shin, J.-H. Ryu, S.-Y. Park, S.-Y. Bae, Thermal stability of fatty acids in subcritical water, Journal of Analytical and Applied Pyrolysis 98 (2012) 250–253, doi:10.1016/j.jaap.2012.08.003.

[59] M. C. Johnson, J. W. Tester, Lipid Transformation in Hydrothermal Processing of Whole Algal Cells, Industrial & Engineering Chemistry Research 52 (32) (2013) 10988–10995, doi:10.1021/ie400876w.

[60] L. Rodolfi, G. Chini Zittelli, N. Bassi, G. Padovani, N. Biondi, G. Bonini, M. R. Tredici, Microalgae for oil: Strain selection, induction of lipid synthesis and outdoor mass cultivation in a low-cost photobioreactor, Biotechnology and Bioengineering 102 (1) (2009) 100–112, doi:10.1002/bit.22033.

[61] B. Gaweł, M. Eftekhardadkhah, G. Øye, Elemental Composition and Fourier Transform Infrared Spectroscopy Analysis of Crude Oils and Their Fractions, Energy & Fuels 28 (2) (2014) 997–1003, doi:10.1021/ef402286y.

[62] J. Speight, Petroleum Chemistry and Refining, Taylor & Francis, Washington, DC, xiv edn., ISBN 1-56032-587-9, 1998.